N° d'ordre : ....

**UNIVERSITY MOHAMMED SEDDIK BENYAHIA**
**JIJEL**
**FACULTY OF EXACT SCIENCES AND INFORMATICS**

**MASTER'S THESIS**

Presented for obtaining the :

**MASTER'S DEGREE**

**Option:** INFORMATIQUE LEGALE ET MULTIMEDIA

By :

**LOUERRAD ANOUAR**
**KECHACHA AHMED RAMZI**

Subject

# Watermarking in medical imaging

| | | |
|---|---|---|
| M. | Boutefara Tarik | President |
| M. | Hmioud Mourad | Examiner |
| M. | Mahrouk Zahir | Supervisor |

I dedicate this modest work

To my dears *Elyas, Aya, Hadia*

To my friend and partner in this project *Sami*

To my special Squad and Friends ... You know

To everyone who has been there for me

And a special feeling of gratitude to my Mother and Father who supported me every step of the way

*Anoir*

I dedicate this modest work

To my dear father and mother

To my dear sisters *Ibtissem* and *Nihed*

To my friend and partner in this Work *Anoir*

To my freinds and everyone who has been there for me

*Ahmed Ramzi*

# *Acknowledgment*

*We would like to sincerely thank our supervisor Mr Zahir Mahrouk for his support, guidance.*

*And also we would like to thank the jury for agreeing to judge this work.*

# Abstract

Dual-Tree Complex Wavelet Transform (DTCWT) is relatively a recent improvement of the Discrete Wavelet Transform (DWT) with important additional properties like shift invariant and directionality.
In this thesis, we propose a blind watermarking scheme based on Dual Tree Complex Wavelet Transform (DTCWT). Single level DTCWT is applied on host image, it decompose the original image into dual nine subbands. by modification on singular value decomposition (SVD), Eigen values of the selected subband are replaced by the Eigen values of the selected subband of the watermark which is multiplied by an appropriate strength factor.
DTCWT provides higher capacity than the real wavelet domain. Modification of the appropriate sub-bands leads to a watermarking scheme which favorably preserves the quality. The additional advantage of the proposed technique is its robustness against the most of common attacks. Analysis and experimental results show much improved performance of the proposed method in comparison with the Hybred method SVD-DWT.

***Keywords :*** *DTCWT, DWT,SVD ,Watermarking.*

# Résumé

La transformation en ondelettes complexes à deux arbres est une amélioration relativement récente de la transformation en ondelettes discrètes avec d'importantes propriétés supplémentaires telles que l'invariant de décalage et la directionnalité.
Dans cette thèse, nous proposons un schéma de filigrane aveugle basé sur la transformation en ondelettes complexes à double arbre (DTCWT). DTCWT à un seul niveau est appliqué sur l'image hôte, il décompose l'image d'origine en deux neuf sous-bandes. par modification de la décomposition des valeurs singulières (SVD), les valeurs Eigen de la sous-bande sélectionnée sont remplacées par les valeurs Eigen de la sous-bande sélectionnée du filigrane qui sont multipliées par un facteur de force approprié.
DTCWT offre une capacité supérieure à celle du domaine d'ondelettes réel. Modification des sous-bandes appropriées conduit à un schéma de filigrane qui favorise préserve la qualité. L'avantage supplémentaire de la technique proposée est son robustesse contre la plupart des attaques courantes. Analyse et résultats expérimentaux montrer des performances nettement améliorées de la méthode proposée par rapport à la méthode Hybred SVD-DWT.

***Mots-clés**: DTCWT, DWT,SVD ,filigrane*

# CONTENTS

# LIST OF FIGURES

# LIST OF TABLES

# ACRONYMES

| | |
|---|---|
| **MRI** | Magnetic Resonance Imaging |
| **SNR** | Signal to Noise Ratio |
| **CNR** | Contrast to Noise Ratio |
| **EPR** | Electrounic Patient Record |
| **SSIM** | Structural similarity indes |
| **PSNR** | Peak Signal to Noise Ratio |
| **MPSNR** | Masking based Peak Signal to Noise Ratio |
| **IWT** | Integer Wavelets Transform |
| **QR** | Quick Response |
| **HIS** | Hospital Information Systems |
| **PID** | Patient Identification Details |
| **LSB** | Least Significant Bit |
| **ISB** | Intermediate Significant Bit |
| **DCT** | Discrete Cosine Transform |
| **DWT** | Discrete Wavelet Transform |
| **IDCT** | Inverse Discrete Cosine Transform |
| **WT** | Wavelet Transforms |
| **HVS** | Human Visual System |
| **CWT** | Complex Wavelet Transform |
| **SVD** | Singular Value Decomposition |
| **ISVD** | Inverse Singular Value Decomposition |
| **FT** | Fourier Transform |
| **DT CWT** | Dual-Tree Complex Wavelet Transform |
| **IDT CWT** | Inverse Dual-Tree Complex Wavelet Transform |
| **IDE** | Integrated Development Environment |
| **DST** | Discrete Sinusoidal Transform |
| **FIR** | Finite Support Filter |
| **GPU** | Graphics Processing Units |
| **MSE** | Mean Squared Error |

# INTRODUCTION

The development of web innovation has expanded the sharing and transmission of digital data. Because of this, it requested the need of systems and techniques to avoid the altering and unlawful appropriation of these information. One of the methods utilized to accomplish copyright security as well as legitimacy of computerized information is digital watermarking which plays a major role in multimedia security tools.
Watermark, which is usually some information related to original data, is inserted in the original data, then the watermarked data is distributed throughout computer networks. Considering the applications of such systems, the watermark can be extracted from the media.
Novel watermarking techniques are classified into two major types, Spatial domain technique and Transform domain technique. In Spatial domain technique, pixel value is directly modified to embed the secret information. The Transform domain technique, works by transforming Original image into transform coefficients by using various popular transforms like DCT, DFT, DWT and DTCWT etc. Transform coefficients are modified to embed the secret data. Transform domain technique achieves more robustness as compared to spatial domain technique but it needs more computational complexity.
Therefore Embedding of secret data in frequency domains has its own advantages and disadvantages. While the embedding of the watermark increases the robustness with respect to image distortions, which is a crucial criteria for medical images and demands a high level of image quality against any type of attacks like filtering, lossy-compression, geometrical distortions.
Medical image watermarking technology hides patients' personal data in the corresponding host medical image, there by protecting patients' privacy and ensuring the safe transmission of this information. However, medical images have their unique characteristics. Medical images are single-channel, grayscale images. The slight change in highly similar background tissues may represent a certain disease. Any subtle change may cause distorted medical images and affect diagnosis. Therefore, the particularity of medical images makes it difficult for traditional medical image digital watermarking algorithms to solve these problems.

This thesis is organized into three chapters
In the first chapter we introduce spiking medical image watermarking, its characteristic,

types, importance and advantages, after that we present model, classification and application of watermarking
In the second chapter we present the basic notions of the wavelet transform on precision the complex wavelet transform CWT, advantages and dual tree complex wavelet transform DT CWT, also Singular Value Decomposition SVD and its watermarking method , properties and advantages.
the results of our method are shown in the third chapter.

# CHAPTER 1

# MEDICAL IMAGE WATERMARKING

## 1.1 Introduction

During last few decades of twentieth century, medical imaging experienced the development of new technologies such as MRI imaging, digital subtraction angiography, Ultrasound imaging...etc
At present, medical imaging infrastructure produces medical images in digital format, which allow transmission and storage of digital medical images and their related information, e.g., patient's data, medical doctor's data, health care centers... The medical file of a patient is composed by clinical examinations, diagnostics, prescriptions and digital images of several types that are stored in the electronic patient record (EPR).
Digital watermarking has recently emerged as a suitable solution to solve some of the problems associated with the management of medical images.
In this chapter, we'll talk about different characteristic and types of medical imaging, after that, we will talk about watermarking and its characteristics, advantages, models, classification and applications.

## 1.2 Medical imaging

### 1.2.1 Definition

Medical imaging, also known as radiology, is the field of medicine in which medical professionals recreate various images of parts of the body for diagnostic or treatment purposes. Medical imaging procedures include non-invasive tests that allow doctors to diagnose injuries and diseases without being intrusive

## 1.2.2 Characteristic

### 1.2.2.1 Size

In medical imaging, the size of the images most often depends on the sensor entering acquisition and the anatomical region to be images. Generally in CT, the images are 512 × 512×12 bit. In MRI the image formats vary more than any other modality with square and non-square matrix formats (e.g. 64 x 64, 64 x 128, 128 x 128, 128 x 192, 256 x 512, 512x512, 512x1024, ...) [1] Each modality has different abilities to solve fine details in a patient's body. Generally two definitions are given to the spatial resolution. In [2], the resolution refers to the ability to see small details. In [3], it represents the capacity of a system of imagery to represent distinctly two objects that are smaller and closer together. According to these definitions, an imaging system has a greater spatial resolution if it can demonstrate the presence smaller and smaller objects in the image. Depending on each modality, one or more factors may cause a limitation of spatial resolution. In the case of MRI images, for example, the Spatial resolution limitation is related to the physical properties of the sensors. Indeed The length The longest MRI wave measures about ten billionth of a meter. However, Sensors fail to represent all this information. Some terms and conditions have a temporal resolution. This represents the number of frames acquired per second. It may vary from 50 frames per second in one frame per second ultrasound in MRI [2]

### 1.2.2.2 Noise

In the field of signal and image processing, the noise corresponds to a random phenomenon which is superimposed in the ideal image. Probably the best approach for to understand noise is to realize that if we acquire several times the image of the same object, motionless and unchanged, we will not observe exactly the same result: the difference is related to the noise. Similarly, by running several times a die, we do not obtain the same result; it's random (Figure 1.1)

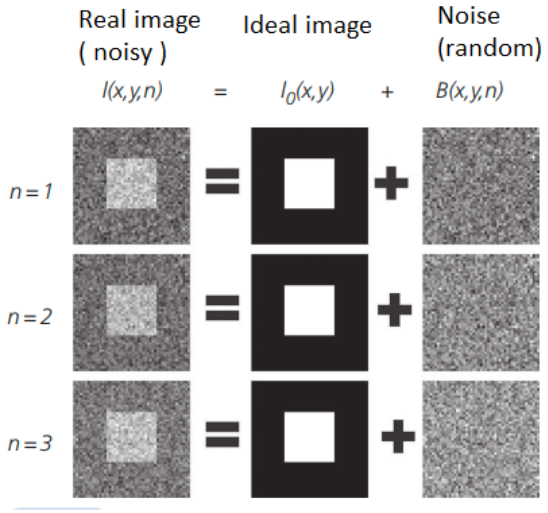


Figure 1.1: Noise

Like any random phenomenon, noise is characterized by its standard deviation (square root of the variance), which we note σ. To quantify the noise level, one generally compares the signal intensity with the standard deviation of the noise for determine the signal-to-noise ratio (SNR):

$$SNR = \frac{S}{\sigma}$$

Where S is the signal strength. Image noise may interfere with interpretation and, in the extreme, make the images completely unreadable. The presence of noise will also deteriorate the spatial resolution since it may be impossible to distinguish structures that are too small in a very noisy (figure 1.2).

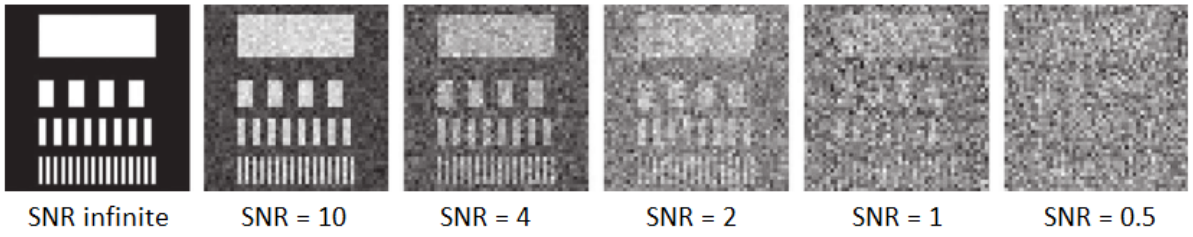


Figure 1.2: Level of SNR

#### 1.2.2.3 Contrast

A diagnosis is usually made by discerning the signal abnormal of a lesion within a normal organ. This is therefore the contrast between the two which allows the diagnosis. If we denote S1 the lesion signal and S2 the background signal, contrast is traditionally defined as:

$$C = \frac{|S1 - S2|}{S1 + S2}$$

A signal of 6 on a background of 2 therefore gives a contrast of 0.5. However, on a digital image, it is easy to change the contrast at will. In the previous example, if we subtract the value 4 from the image, the two previous values become respectively +2 and 2 with a contrast which becomes infinite, etc. More attractive is therefore to consider the contrast-to-noise ratio (CNR):

$$CNR = C = \frac{|S1 - S2|}{\sigma}$$

### 1.2.3 Types

#### 1.2.3.1 Radioactivity

Nuclear scintigraphy techniques rely on the use of a tracer Radioactive that emits detectable radiation from measuring devices. These Radiopharmaceutical molecules are chosen to attach preferentially to some cells according to the type of diagnosis desired. Computer processing of The data then allows the spatial origin of these radiation to be

reconstructed and Deduce the areas of the body where the plotter focused. The image obtained is the most often a projection but it is possible to obtain a 3D cut or reconstruction of the plotter distribution. In the United States, in 2010, the FDA decided to tighten its control, considering that tomography and fluoroscopy expose more than necessary some patients with ionizing radiation; according to the american institute of cancer, theseOverdoses would induce an additional 29,000 cancers/year and 15,000 deaths in the country. [4]

#### 1.2.3.2 MRI

MRI are electromagnetic waves of the same nature as waves light but more energetic. They have the property of being attenuated by all kinds substances including liquids and gases. They can go through the human body, where they will be more or less attenuated depending on the density of the structures traversed. [4] The use of MRI is common. These rays, like the rays gamma are ionizing and therefore dangerous. In particular, the irradiation of a cell in The mitosis phase can cause a mutation in DNA and can cause the appearance of cancer at term. However, through radiation protection measures, the inherent risk X exams is limited to the maximum. Different types of examinations use MRI:
- MRI, using x-rays and sometimes injecting contrast media. The images obtained are projections of the organs and the different systems according to a plan. Radiography is generally used for the bone system because it is the most visible system on a body MRI.
- MRI scanner, MRI tomography. millimeter (or infra-millimeter) that can be studied in all space, as well as three-dimensional images.
- DEXA scanner measuring bone density .

Figure 1.3: MRI

#### 1.2.3.3 Scintigraphy

Scintigraphy uses a small amount of radioactivity to make images (hence the name nuclear medicine). It allows you to visualize how a organ (heart, lungs, bladder kidneys, digestive

organs) or whole system (system osteoarticular, endocrine system, immune system...). It allows the "labeling" of certain molecules of the organism, to study their circulation in the body (for example, white blood cell scintigraphy). Tagged cells can be visualized. [4]

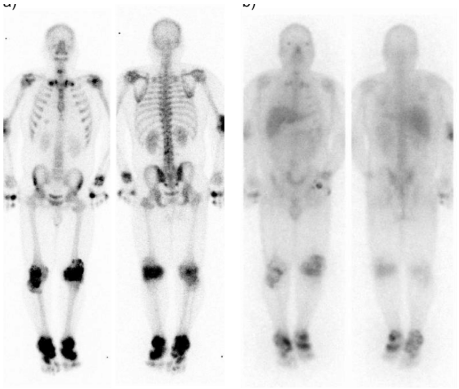

Figure 1.4: Scintigraphy

### 1.2.4 Importance of medical image

Medical imaging has been ranked as one of the top medical development of the past 1000 years by the New England Journal of medicine and various other peer-reviewed journals , it is absolutely necessary when tracking the progress of an ongoing illness. MRI and CT scans allow the physician to monitor the effectiveness of treatment and adjust protocols as necessary. The detailed information generated by medical imaging provides patients with better, more comprehensive care.

## 1.3 Medical image watermarking

### 1.3.1 Digital image watermarking

Digital image watermarking is inserting a secret related data or information, into a cover image, this data cannot be removed or replaced by any intruder without authorization.

### 1.3.2 Medical image watermarking

In the case we are interested in, medical image watermarking case, we embed secret data for instance Electronic Patient Record EPR such as patient name, age, sex, demographic information and diagnosis result, along with logo and digital signatures of radiologist and clinician into a cover medical image like Radiography, ultrasound, MRI. . . etc. The goal is to communicate between hospitals safely and effectively.
This watermark should be detectable and extractable from the host image while preserving its quality during these processes.

### 1.3.3 Characteristic

Medical image watermarking need three main features and properties

#### 1.3.3.1 Robustness

Robustness of the watermark is the resistance of the watermark against malicious attacks that are preformed by expert attackers in aim to remove, replace or distort the watermark. The watermark system should also be resistant against innocent attacks like spatial domain operations (compression, median filtering... etc.), geometric operations including rotation, cropping, cutting... etc. It includes other operations such as scanning, printing, enhancement or even during transferring or distribution (telemedicine).
The robustness of a medical image watermark is important and necessary in case of detection of the watermark by intruders so it can be resistible against their removal and distortion attacks that aims to remove image or destroy the inserted data from the image. We classify the watermark based on its robustness into three categories: robust, semi-fragile, and fragile as we will see later.

#### 1.3.3.2 Imperceptibility

Imperceptibility is an essential condition in evaluating the performance of a watermarking system, states that the visual similarity and the degradation of quality between the original and the watermarked image should be indistinguishable by the human eye after embedding the watermark, considering the major human perceptual system functions (luminance, contrast and structure) or the watermark value will be lost. Different methods for evaluating the imperceptibility of the watermark are used such as Structural similarity index (SSIM) or Peak-signal-to-Noise ratio (PSNR) and its improved versions Masking-Based Peak-signal-to-Noise ratio (MPSNR) which preformed better in evaluating the visibility of the watermark [5].
There are two main reasons of the importance of the invisibility factor in medical image: medical images such as radiology or MRI contains important and sensitive data, so does their related inserted watermark and any bad degradation of quality effects this data causes it to lose its value and can be pose a danger of the patient's health in case of distortion.
The perceptible watermark that introduces its location into detection, provides easy access to malicious attackers to extract, alter, or even remove the imbedded secret data, and poses a threat to the patient's privacy and life.

#### 1.3.3.3 Capacity

Capacity or payload is the quantity (number of bits) of the embedded data into the host image, this quantity should be as high as possible. However inserting more watermark information is difficult without causing more distortion and compromising other watermark features, which is not tolerable in military and medical applications.
The watermarking capacity is determined by the watermark encoder and decoder, the available information to attackers, the statistical model used in the host image and the distortion limitations of the image [6].
In the medical field, Electronic Patient Record EPR should be inserted into the cover medical image without affecting its quality, while satisfying watermarking robustness and imperceptibility..
For the purpose of preserving the watermark quality, watermarking techniques must be

implemented to minimize this distortion such as the combination of bit-plane method, integer wavelets transform IWT and Quick Response QR code, where the watermark is converted into a QR code, reducing the capacity [7].
Satisfying the capacity, imperceptibility and robustness of the watermark simultaneously is impossible, due to their conflicting characteristics. For instance a watermark imperceptibility may be decreased by increasing the properties of robustness and capacity, and vice versa. Therefore a good trade-off must be maintained between all three characteristics, combining various techniques in different domains to fulfill the requirements. [8].
.

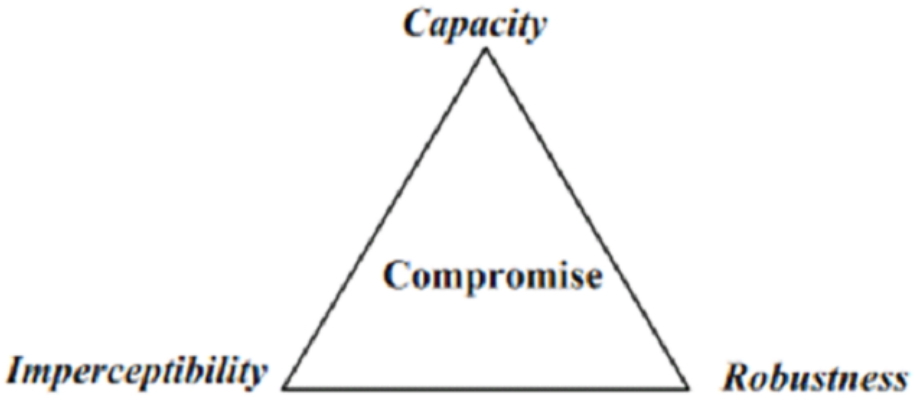


Figure 1.5: Triangle robustness, imperceptibility and capacity.

### 1.3.4 Advantages of medical image watermarking

Watermarking has received much attention recently for medical image applications because of its various attractive attributes [9] [10] [11], which are listed below:

#### 1.3.4.1 Security and privacy

The fundamental and most attractive property of watermarking is data hiding capability [12] [13]. The utmost confidentiality can be maintained by hiding the secret data into the images. Keeping necessary medical data (e.g., EPR including demographic data, diagnostic results, treatment procedures etc.) hidden in medical images may give a better security against vicious tampering assuming medical images would not be of people's interest without the patient information [14] [15]. Indeed that's tampered designedly or in an unintended manner, can be detected and conceivably recovered by using an applicable watermarking scheme [16] [17]. Hence, Coatrieux etal. [9] outlined three main objects of watermarking in the medical image operations data hiding, integrity control, and authenticity, which can give the needed security of medical images. For illustration, data-hiding ideal of watermarking allows fitting meta-data and other information so that the image

is more useful or easier to use. Integrity control ideal of watermarking ascertains that the image has not been modified in an unauthorized manner. Digital watermarking allows endless association of image content with attestations of its trustability by modifying some image pixel values, singly of the image train format. It can also operate in a stand- alone terrain and has a protean communication set. In addition, authenticity traces the origin of an image.

#### 1.3.4.2 Avoiding detachment

The data hiding property of watermarking mentioned above farther facilitates reflection of necessary information to avoid detachment. Millions of medical images are being produced in radiology departments around the world, which have immense value to rehearsing medical professionals, medical experimenters, and scholars. Inquiries in this field are being Fulfilled to bed patient data to medical images [12] [18] [19]. If the EPR and the images are separate, the chance of detachment of patient data from the image becomes advanced. Losing a data will be veritably pivotal in the case of medical image. In order to avoid this misplacing or detachment, watermarking offers necessary data embedding within the image itself.

#### 1.3.4.3 Indexing

Another benefit stems from data hiding capability of watermarking is indexing, where applicable keywords or indicators can be bedded into the images and used for effective archiving and reclamation of the images from databases [10].

#### 1.3.4.4 Non-repudiation

Distribution of the watermarked images between HISs may beget nonrepudiation problem, where both the involved parties (e.g., sanitarium help and clinician) may repudiate that they didn't shoot the data. Along with other advantages, watermarking is also promising to support nonrepudiation in colorful multimedia operations [20] [21]. Hence, use of a keybased watermarking system may grease nonrepudiation in teleradiology similar that both parties could be in safer side; where crucial used by the sanitarium could be their ensigns or digital autographs.

#### 1.3.4.5 Controlling access

Provision for using keys in watermarking schemes further provides an volition to access control medium, where nonpublic meta-data can be penetrated with the proper authoritative rights given in terms of keys [10] [22].

#### 1.3.4.6 Memory and bandwidth saving

Memory and bandwidth saving Storage space and bandwidth conditions are important decisive factor for small hospitals fiscal frugality. The memory for storehouse can be saved to a certain extent in Hospital Information Systems (HIS) by bedding the EPR in the image [19] [23]. On the other hand, huge quantum of bandwidth is needed for the transmission of the image data in teleradiology. The fresh demand of bandwidth for the

transmission of the metadata can be avoided if the data is hidden in the image itself. Since the EPR and the image can be integrated into one, bandwidth for the transmission can be reduced in telemedicine operations [10].

### 1.3.5 Need of watermarking for medical image

The exchange of databases between hospitals requires an effective transmission channel to reduce the cost of health care. This exchange involves transmission of a large number of different vital patient information in the form of graphs, word documents or medical images. When the transmission is done independently using internet or other mediums, the transmission time and cost and also the unauthorized access may be passed. With the development of the Web Technology and the Ecommerce, it's clear that digital content ( textbook, image, audio, videotape etc) protection has come an important issue. Digital watermarking has been proposed an approach to increase medical image security, integrity and confidentiality. Medical image watermarking is one of the subcategory of image watermarking in the sense that images have special conditions. In the digital watermarking fashion, the factual bits are scattered in the image in such a way that they can not be linked and show adaptability against attempts to remove the retired data. Still, in practice, the watermarking algorithms should be combined with a secure and effective brand protection protocol to insure the brand protection in case of any disagreement. Uprooted watermarked medical images shouldn't differ from their original dupe, because the clinical reading of the images shouldn't be affected. Currently, Internet is being extensively used for the purpose of creation and distribution of medical content over the internet. An electronic case record (EPR) is a wide conception which is defined as a collection of electronic health information about individual cases or populations. A record in digital format are maintained and participated between different health care centers. In utmost of the cases this sharing can do by way of network- connected enterprise-wide information systems and other information networks. EPRs may involve a range of data, including medical history record, drug and disinclinations, immunization status record, laboratory test results, radiological images, vital signs, particular statistics like age and weight, and billing record also electronic medical data may include chancing new drags and scientific exploration, Hospitals and medical health care centers have huge databases including medical images, textbook document and case records. Utmost of the former inquiries have concentrated on conserving the resolution of the medical images after bedding the watermark without testing the robustness and irreproachability of the schemes against colorful attacks [24]

## 1.4 Watermarking model

Watermarking involves two fundamental steps Embedding phase and the Extraction phase

### 1.4.1 Embedding phase

It consists of the insertion of data into the cover image which needs to be pre-processed. Then, its entropy is evaluated to localize the integrating capacity information of the image.

Then, using the encoder, the watermark is embedded into the high entropy value in an imperceptible way to the human eye respecting the fundamental characteristics of the watermark and the watermarking method used. [8]
The encoder generally contain three components or inputs producing the watermarked image “I w ” as an output
- Host image “I ” to be watermarked
- Watermark W to be inserted in the cover image
- Encryption Key K to enforce the security of the watermark

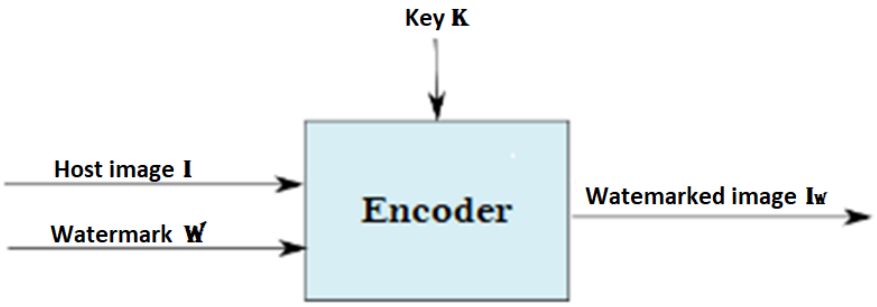


Figure 1.6: Embedding process.

In medical image watermarking, we insert and encrypt a Patient Identification Details PID to identify the patient in case of transmission between clinics or hospitals, along with the watermark W as generally an Electronic Patient Record EPR [25].

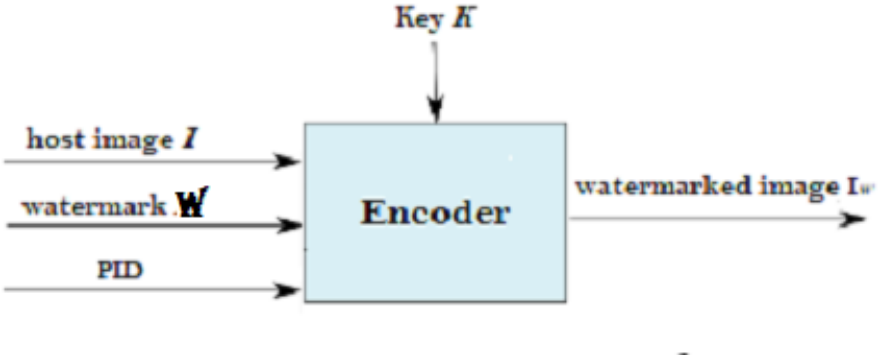


Figure 1.7: Embedding process.

Generally the watermark is embedded into the host image using one of two different methods: additive and subtractive

#### 1.4.1.1 Additive embedding

This method gives the ability to recover the original image during the extraction of the watermark [26], applied by Adding the watermark W directly to the host image I, modifying

and lowering the energy of the components: watermark W and an optional Encryption key K by multiplying them with small weighting coefficients in order to make them invisible producing a linear mixture..

$$\mathbf{Iw = I + aK + bW\ (1)}$$

Where “a” denotes small weighting coefficients and “b” denotes small filter coefficients convoluted with the watermark
the paper of [27] illustrates this method of embedding scheme where the host image “Cameraman” is watermarked using (1), where the components are a key image and a watermark image in spatial domain..

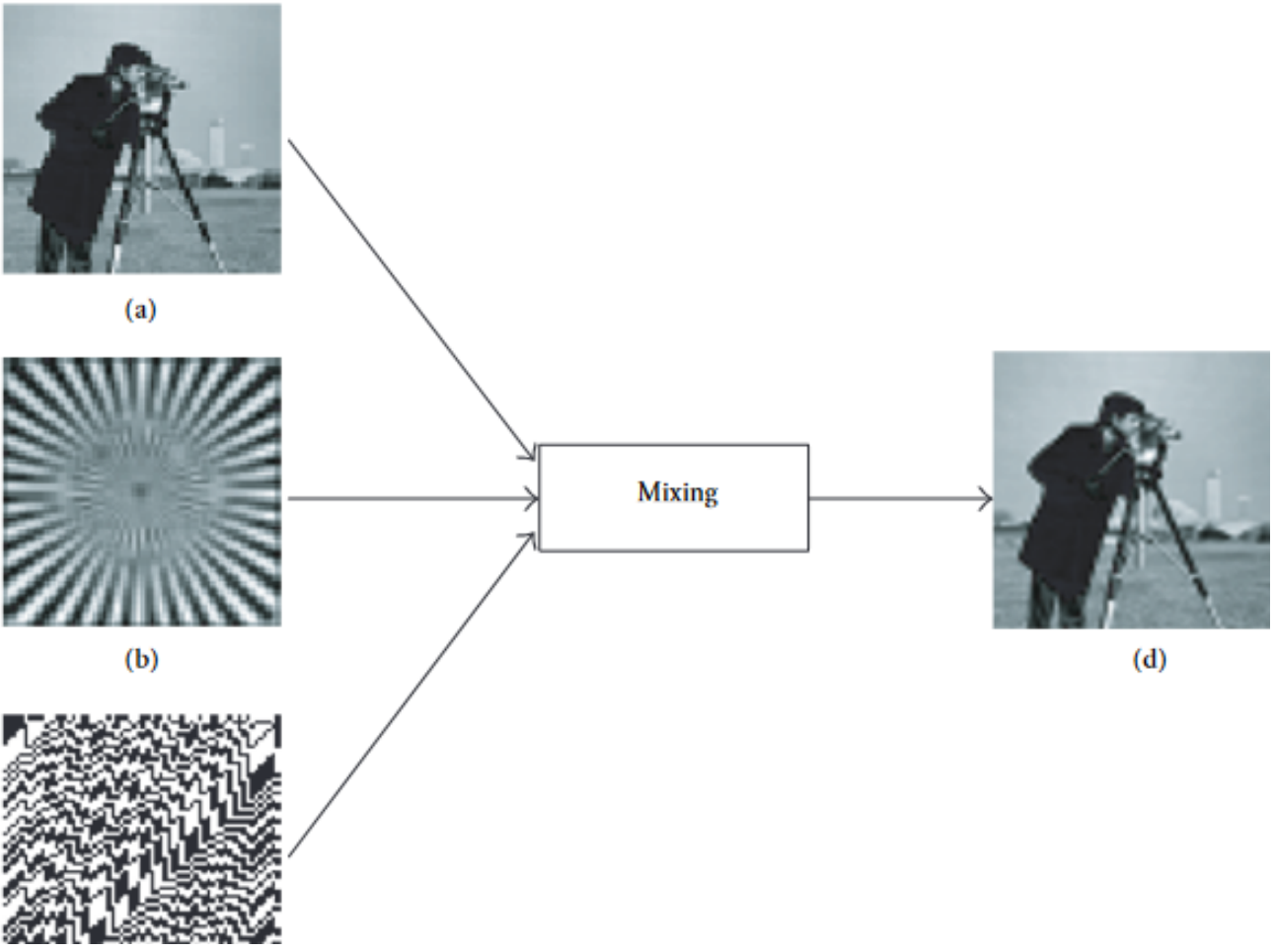


Figure 1.8: (a) Cameraman (original image), (b) Secrete key image, (c) Watermark image (Gold-like sequence),(d) Watermarked image.

The paper of [28] also illustrates the additive embedding process, the process in the multi-resolution domain and without using the Encryption key K based on the following function:

$$\mathbf{I(i,j) = I(i,j) + (\ \alpha\times\ W(i,j))\ (2)}$$

Where I is the DWT coefficient of the original image I and is also the watermarked image Iw, αdenotes weighting coefficient, while W is the DWT coefficient of the watermark.

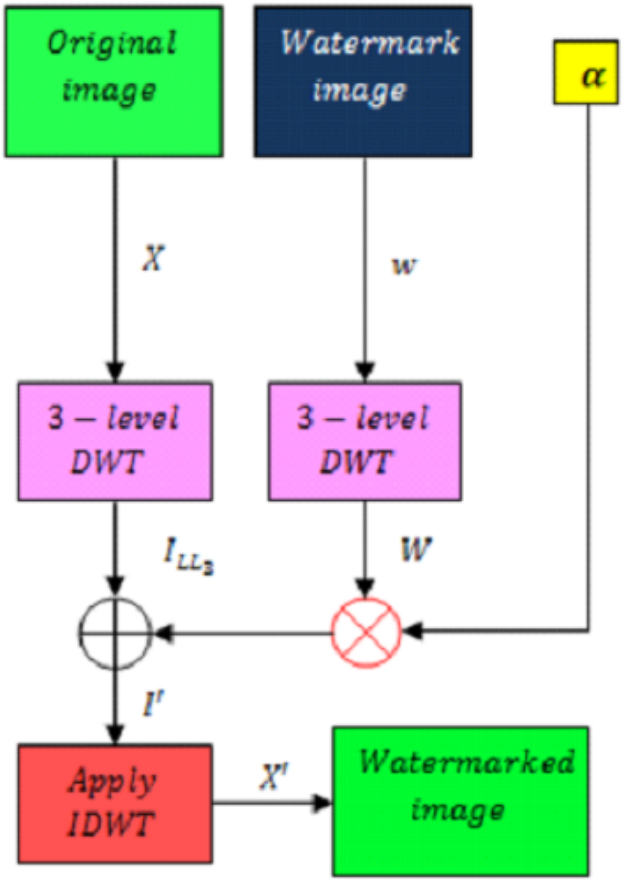


Figure 1.9: DWT additive watermarking system

After applying the DWT to the watermark, and obtaining its coefficients, The watermark coefficients are embedded into LH3 sub-band of the original image, the value of the pixel is modified directly using the formula (2). then, inverse wavelet transform IDWT is applied to obtain the watermarked image.

#### 1.4.1.2 Subtractive embedding

Subtractive embedding means the loss of the original image by replacing an information of the cover image with a new a new information (watermark), original data cannot be recovered after the watermark extraction process. This method helps with a permanent association of the watermark to allow continuous protection of the watermarked images. This method does not keep the original bit-planes or RONI pixels that are replaced for embedding, and thus reduces the side information overhead.
As far as we searched, this method is rarely used in the literature, because of its disadvantage of not able to recover the original image, which is critical and necessary in some fields such as the military or the medical field.

The simplest subtractive method is using LSB, The watermark is inserted into the least significant bits of the host image and can be extracted in the same way. An example of LSB would be :
Suppose two pixel values in the host image are 140 (10,001,100) and 130 (10,00 0,010). Then, using the LSB technique, if the embedded watermark is 10, then he watermarked pixel values will be 141 (10,001,101) and 130 (10,00 0,010).

### 1.4.2 Extraction phase

The process composed of:
- Detect the presence and location of the information W from the watermarked image Iw.
- Extract the watermark W and reconstruct the original image I, without any loss of information which is the reverse process of the embedding procedure.
The decoder or extraction process have as an input two necessary components
- The watermarked image Iw
- The encryption/decryption key K

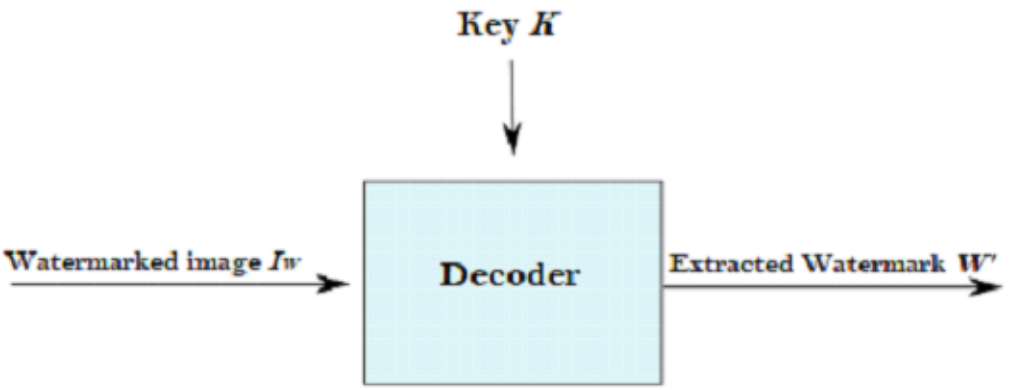


Figure 1.10: Extraction process

## 1.5 Watermarking Classification

Digital image watermarking depend on the type of working domain (spatial, frequency) and the fragility of the watermarking system (robust, semi-fragile, fragile). This section analyzes these mentioned watermarking methods.

### 1.5.1 Based on the Domain

#### 1.5.1.1 Spatial Domain

In these methods, the watermark is inserted directly into the cover image by modifying the pixel values of the original image. Spatial domain algorithms are simple, fast, low complex and offer high embedding capacity in addition to the capability of embedding

multiple small watermarks. The main disadvantage is its inability to survive against many operations such as lossy compression, noise adding. . . , in addition it's fragile against unauthorized removal attacks.

**Least Significant Bit (LSB):**

Least significant bit is the simplest spatial domain technique, the watermark is inserted into the least significant bits of the cover image and can be extracted the same way. This changes are not visible to the human eye and causes a negligible impact on the host image because it carries less relevant information. However, this technique is easily effected by simple image operations such as compression, cropping, noise addition. . . , and may be attacked by hackers easily modifying the LSB bits to "1", altering the embedded watermark.

The four least significant bits (i.e., the fifth–eighth bits of the cover image) can be replaced with the chosen bit of the watermark by using an OR operation [29]. This method first converts the host image into a stream of binary bits, outputs zero in the embedded bit, and then shifts the secret image to the right by 4 bits. Then, an OR operation is performed on the cover and watermark to obtain the watermarked image.

An example as described in the figure . Let the pixel value of the cover image (or host image) be 131 (10,000,011) and the binary representation of the secret image (Watermark) be (11,110,000).

After embedding out zero, the cover image value is 128 (10,000,000). After shifting right by four bits, the secret image value is 15 (00,001,111). Then, an exclusive OR operation is done to obtain the watermarked image pixel, which has a value of 143 (10,001,111)

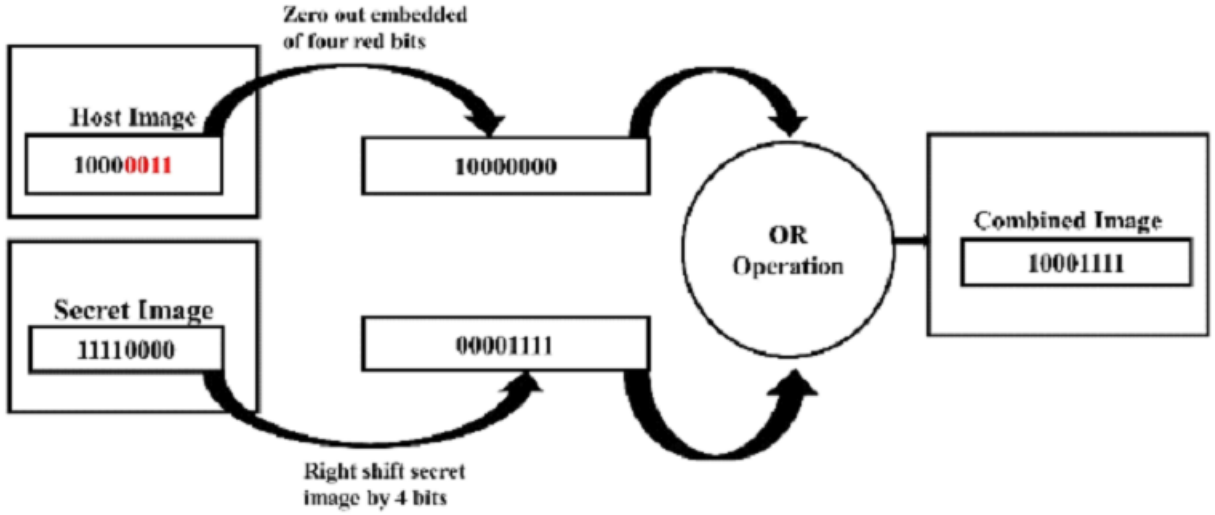


Figure 1.11: LSB

**Intermediate Significant Bit (ISB):**

In intermediate significant bit (ISB). the watermark pixel's position has been tested according to the range of each bit- plane. Therefore, if the position of watermarked pixel is in the middle of the range, any effect on the pixel by attacks will make it delicate to move the named bit to other range. Meanwhile, if the pixel value is located at the edges of the ranges, any small change caused by attacks will move the pixel from a range to other

range, and the watermark can not be extracted. [30] tried to find the best pixel value, in between the middle and the edge of the range that can secure the watermark object from several kinds of attacks, and at the same time keep the watermarked image at the minimal deformation. This was achieved by situating the watermarked pixel down from the edge of the range, all possible positions of pixel between the middle and the edge of the range were tested to find the best pixel value (threshold value), which was institute to be at the 4th bit- plane with a bias value = 6 (the bias value is the distance between the position of the watermarked pixel and the edge of the range) [30]. ISB techniques can be used, instead of LSB techniques , where the secret message can be embedded in a bit-plane (or bit-planes) [31]

#### 1.5.1.2 Frequency Domain

Transformation techniques are applied to the original image before embedding the watermark provide more robustness against various image processing attacks compared to the spatial domain techniques. These methods generate the transform domain coefficients of the cover image I using a predefined transform. Then, it embeds the watermark W by changing these coefficients. The most popular transform domain techniques utilized in watermark embedding are Discrete Cosine Transform DCT, Discrete Wavelet Transform DWT. Finally, it extracts the watermark W, with the help of the key K, using an inverse transformation. [8]

**Discrete Cosine Transform DCT**

The discrete cosine transform (DCT) is widely used in digital image watermarking since it has strong robustness, it separates an image into its equivalent frequency coefficients by modifying frequency components, which can be expressed as a sum of cosine functions. The DCT is important for image compression; for instance, in the JPEG image format. The one-dimensional (1D) DCT is defined by the following equation [8]

$$y(k) = \alpha(k) \sum_{n=0}^{(N-1)} x(n) \cos \frac{\pi(2n+1)k}{2N}, k = 0, 1, ..., N-1$$

And the inverse transform IDCT is given by:

$$x(n) = \sum_{k=0}^{(N-1)} \alpha(k) y(n) \cos \frac{\pi(2n+1)k}{2N}, n = 0, 1, ..., N-1$$

With

$$\alpha(0) = \sqrt{\frac{1}{N}}, k = 0 and \alpha(k) = \sqrt{\frac{2}{N}}, 1 \leq k \leq N-1$$

Where N is the number of given data samples: x(0),..., x(N  1), x(n) is the input data

sample, y(k) is the DCT coefficient, and $\alpha$(k) is the scaling factor.

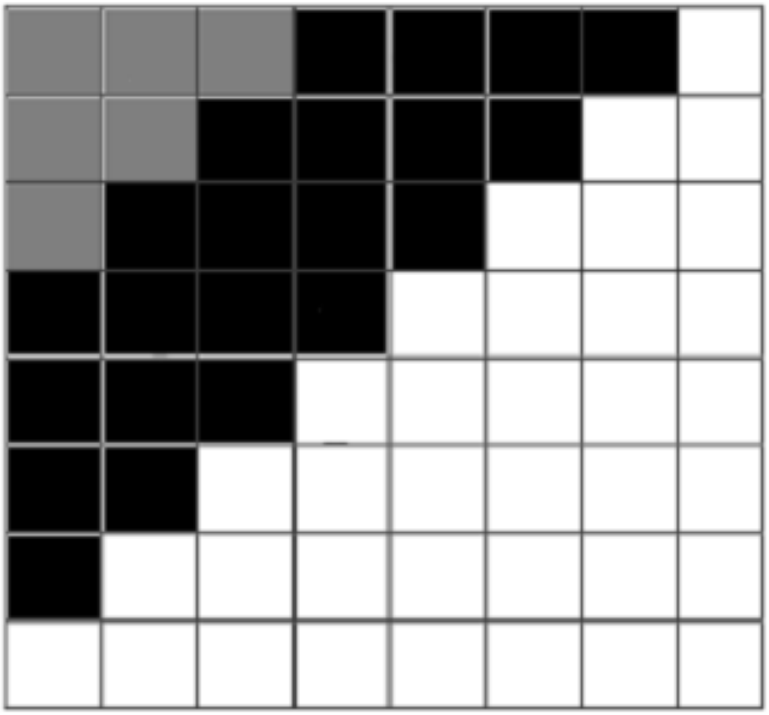

Figure 1.12: DCT decomposition of an image

Based on many studies, embedding the watermark information require dividing the image into different frequency bands and insert the watermark into a selected region as shown in the figure above. The gray color denotes the lowest frequency component of the block, while the white color denotes high frequency component and the black color denotes middle frequency component. To obtain the watermarked image by applying the inverse Discrete Cosine Transform (IDCT).

**Discrete Wavelet Transform DWT**

For any watermarking system there are three requirements: robustness, imperceptibility, capacity. it is required to develop a robust watermarking algorithm that in the same time preserves the visual quality of the host image after being watermarked. the developed watermarking algorithm is also required to fulfill capacity requirement.

Discrete wavelet transform DWT has its own characteristics that enable to develop a robust watermarking algorithm that saves the visual quality of the watermarked image.

Discrete wavelet transform DWT of the image produces multi resolution representation of an image. The multi resolution representation provides a simple framework for interpreting the image information. The DWT analyses the signal at multiple resolution.

It divides the image into high frequency quadrants and low frequency quadrants. The Low frequency quadrant is again split into two more parts of high and low frequencies and this process is repeated until the signal has been entirely decomposed.


Figure 1.13: 2-level discrete wavelet decomposition

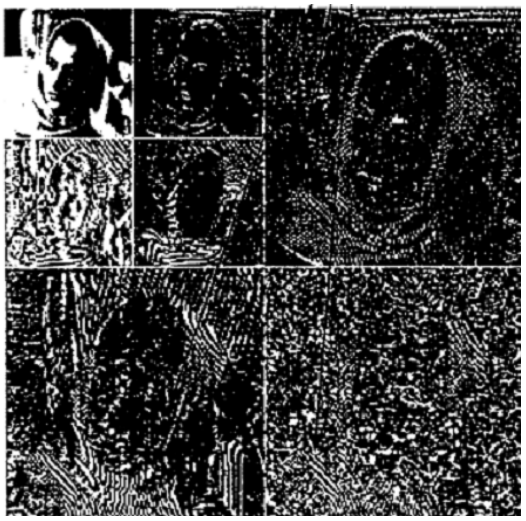

Figure 1.14: 2-level Dwt decomposition of an image

**- Functioning**

In two dimensional applications, for each level of decomposition, we first perform the DWT in the vertical direction, followed by the DWT in the horizontal direction. After the first level of decomposition, there are 4 sub-bands: LL1, LH1, HL1, and HH1. For each successive level of decomposition, the LL sub-band of the previous level is used as the input. To perform second level decomposition, the DWT is applied to LL1 band which decomposes the LL1 band into the four sub-bands LL2, LH2, HL2, and HH2. This results in 7 sub-bands per component. LH1, HL1, and HH1 contain the highest frequency bands present in the image, while LL2 contains the lowest frequency band [32].

The low frequency coefficients are more robust to embed watermark because it contains more information of the original image.

The high frequency part contains information about the edge components, The high frequency components are usually used for watermarking since the human eye is less sensitive to changes in edges.

The reconstruct of the original image from the decomposed image is performed by IDWT.

The digital wavelet transform are scalable in nature. DWT more frequently used in digital image watermarking because of its excellent spatial localization and multi resolution techniques. The excellent spatial localization property is very convenient to recognize the area in the cover image in which the watermark is embedded efficiently.

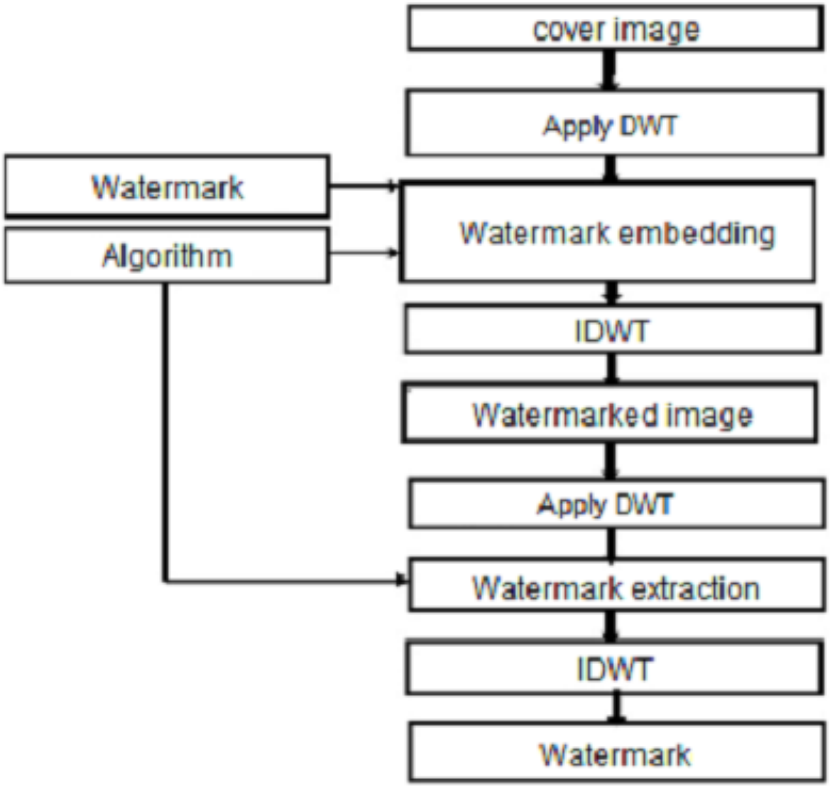


Figure 1.15: DWT image watermarking

The DWT of a signal x[n] is defined by the following equations :

$$W_{\Phi}[j_0, k] = \frac{1}{\sqrt{M}} \sum_{n} x[n]\phi_{j_0,k}[n] \tag{1.1}$$

$$W_{\psi}[j, k] = \frac{1}{\sqrt{M}} \sum_{n} x[n]\psi_{j,k}[n], for j \geq j_0 \tag{1.2}$$

where $W_{\Phi}[j_0, k]$ are the approximation coefficients, $W_{\psi}[j, k]$ are the detail coefficients, and the inverse DWT is given by :

$$x[n] = \frac{1}{\sqrt{M}} \sum_{k} \phi_{j_0,k} \Phi j0, k[n] + \frac{1}{\sqrt{M}} \sum_{j=j0}^{J} \sum_{k} W_{\psi}[j, k]\psi_{j,k}[n] \tag{1.3}$$

with

$$n = 0, 1, 2, ..., M-1, j = 0, 1, 2, ..., J-1, k = 0, 1, 2, ..., 2^j - 1 \tag{1.4}$$

Here M is the number of samples to be transferred = 2J, J is the number of transfer levels, $\Phi j, k[n]$ and ψj ,k [n] are two basis functions, φ[n] denotes the scaling function, and ψ[n] denotes the wavelet function.
Many studies have been carried out on the authentication of images in the DWT domain. For example:
-Chen [33] proposed a digital image watermarking algorithm based on wavelet domain. The algorithm analyzes the complexity of the images concerning imperceptibility and robustness. The method divides the cover image into different blocks, which are selected for embedding the watermark. Then, with the help of the optimal sub-bands, the DWT coefficient is classified based on sub-bands that have lower frequencies. Many experiments were carried out, and the results demonstrated strong robustness and imperceptibility of the system against some common attacks.
-Another paper [34] proposed an efficient digital image watermarking technique based on the wavelet transform for protecting copyright holder information, in which a one-level wavelet coefficient (LL) is generated in the host image, and 8 × 8 blocking operations are used on the grayscale watermark image. For embedding, each block of both images is compared and scaled with a scaling factor α. At the receiver site, the system extracts the watermark image in the opposite manner. The simulation results demonstrated that their proposed scheme is more robust against noise, as compared to existing methods, in terms of PSNR and MSE.
-the paper of [35] proposed a robust watermarking technique based on DWT wavelet transform on the second level (2-level DWT), embedding process contains: applying the 2D-DWT to both host image and watermark image, taking the LL sub-bands of the host and the watermark after being multiplied by a visibility factor, and applying IDWT to obtain the watermarked image. The extraction process is executed the opposite way. The MSE and PSNR results convey the robustness of 2 level discrete wavelet transform compared to 1 level discrete wavelet transform.

**- Characteristics of DWT with Relevance to Watermarking**
The wavelet transform decomposes the image into three spatial directions i.e. horizontal, vertical and diagonal. it reflects the different properties of the Human Visual System (HVS) more precisely .
Larger the magnitude of the wavelet coefficient the more significant it is. Low frequency components have larger perceptual capacity compared to high frequency components, because they have large magnitudes and can be used to embed stronger watermarks. The magnitude of DWT coefficients reduces at each successive level of decomposition (i.e. LL2 , LL3...LLn)

**- Merits of DWT over DCT:**
- DWT gives better visual image quality as compared to the DCT.

- Wavelet transform reflects the HVS more closely and understands the working of HVS more clearly than the DCT
- DWT allows better localization as compared to the DCT.
- The watermarking method is more robust to image compression as well as to other common image distortions like rescaling half toning, additive noise etc...
- DWT defines the multi resolution description of the image. So, the image can be shown in different levels of resolution and proceed from low resolution to high resolution.

## 1.5.2 Based on Robustness

### 1.5.2.1 Robust

Robust watermarking is mainly used for copyright protection. Here robust means the embedded watermark should be resistant to various signal processing operations like scale, crop, compression etc. It should be also hard to detect by the hacker to avoid removal attacks.
In [36] used robust watermarking in the spatial domain. This watermark requires to be: irremovable by an 'attacker', easily and secured detectable by the authorized side, perceptually and statistically invisible, resistant to lossy compression, filtering ... etc.

### 1.5.2.2 Fragile

Fragile watermarking is used for content authentication. A fragile watermark can be altered or destroyed when the digital content is modified, it's intolerable to the smallest modifications, and easy to detect and extract the watermark.
As done in the paper [37], the authors proposed a watermarking system that uses DCT watermarking and a hashing function to preserve the original coefficients. in case of any modification, the watermark extracted will be different than the original, to indicate that tampering has taken place.

### 1.5.2.3 Semi-Fragile

Semi-Fragile watermarking is Robust against authorized attacks, but fragile against the unauthorized operations also used for verifying the authentication of the patient and integrity of the medical images.
The Semi-fragile watermarking system proposed in [38] aims for content authentication, using wavelet coefficients for embedding the watermark, the watermark is fragile to malicious attacks such as filtering, noise..., and robust against JPEG compression. These features that makes the watermarking system semi-fragile.

## 1.6 Watermarking application

### 1.6.1 Authentication and tamper detection

It assures the authenticity of patient information and if any alterations have been applied whether intentional attacks like removal operations or not intentional attacks like filtering, compression, cropping... etc. during transformation from the starting point to the destination.
Fragile, and Semi-Fragile watermarks are the most fitting for this application.

### 1.6.2 Annotation

By incorporating the watermarking mechanism in the different modality machines like CT or MRI scanners, important details can be stored in images imperceptibly and immediately after the production of the images in the radiology departments without affecting the ROI region of the image.
Fragile, and Semi-Fragile watermarks are the best for this application.

### 1.6.3 Patient's private information Integration and protection (Confidentiality, data hiding)

Medical image data hiding is the process of the integration and hiding a set of patient data (name, age, health information... etc.) electronic patient report EPR into a diagnosis image imperceptibly so it does not perceptually distort the image.
The confidentiality of the medical images and reports is very critical so it is essential to efficiently hide the data during transmission.
Robust watermarking is essential in this application to preserve the confidentiality and security of the medical images and its secret data.

## 1.7 Conclusion

In this chapter , we introduced medical imaging such as MRI, Ultrasound, Scintigraphy images ...etc. we also introduced the different characteristics of medical images including their size, noise and contrast. The Importance of medical images was showed which evolved to be a necessity in modern medicine development.
The chapter then presented the technology of digital watermarking and specifically the medical image watermarking, along with the main characteristics of this technology (robustness, invisibility and capacity) and the advantages it provides in the medical field.
We went into the details of the watermarking operation, starting from its model and steps (embedding and extraction),to the important classifications of the watermarking process whether the domain classification (LSB, DCT,DWT ...etc) or the robustness classification (robust, fragile and Semi-fragile), and we finished with the most common medical applications of watermarking.
In the next chapter, we will introduce the CWT and SVD methods.

# CHAPTER 2

# COMPLEX WAVELET TRANSFORMS (CWT) AND SINGULAR VALUE DECOMPOSITION (SVD)

## 2.1 Introduction

The wavelet transform (WT) appeared in the field of image/signal processing as an alternative to Fourier transform (FT) and its associated transforms, namely the discrete cosine transform (DCT) and the transform discrete sinusoidal (DST). A new wavelet transform is the complex wavelet transform (CWT), solves the shift invariance problem and low directional selectivity in two dimensions, which are found in the discrete wavelets transform (DWT). Similar to the adjustable filters, the CWT is a wavelet transform with a limited redundancy of 2d, where d is the number of dimensions in the processed signal.
In this chapter , we will present the basic notions of the wavelet transform on precision the complex wavelet transform CWT and Singular Value Decomposition SVD.

## 2.2 Wavelet Transform WT

Wavelet decomposition distributes signal discontinuities in its locality to multiple scales causing higher amplitudes for wavelet coefficients corresponding to the desired signal, while noise coefficients at several scales are evenly distributed across all scales. This parsimony within the coefficients of wavelets is exploited by estimating a threshold value to distinguish the coefficients corresponding to the noise and the desired signal. The wavelet transform is presented as one of the most effective tools for signal noise due to its representation sparse signal at several scales. Unlike FT and DCT, WT allows a good frequency time localization. In addition, by its nature and construction, the WT allows localization Multi-resolution. The basis used in the WT, can be any function that represents a Compact oscillatory wave that satisfies both conditions:

$$\int_{-\infty}^{+\infty} \psi(t)dt = 0 \tag{2.1}$$

And

$$C(a,b) = \int_{-\infty}^{+\infty} |\psi(t)|^2 dt < 0 \tag{2.2}$$

The wavelet transform breaks down the input signal, equation (2.3), into a series wavelet functions $\psi a$, b(t) that derive from a mother function $\psi(t)$ equation (2.4).

$$C(a,b) = \int_{-\infty}^{+\infty} x(t)\psi a, b(t)dt \tag{2.3}$$

$$\psi a, b(t) = \frac{1}{\sqrt{a}}(\frac{t-b'}{\sqrt{a}}) \tag{2.4}$$

Where a: is the scale factor, b: is the translation factor

– The function $\psi$ must be oscillating and of zero integral.
– $\psi$ must be of integrable square.
– $\psi$ can be of complex values.
– There are many possible parents wavelets.
– Approximate the continuous Fourier transform.
– Wavelet transformation is a linear transformation

The transform is calculated by continuously moving a constant-scale function on the signal, the coefficients of the transform are very redundant. To make the calculation more convenient, we use the discrete wavelet transform (DWT), obtained by sampling of the CWT. It is not necessary to explicitly calculate the wavelet shape and scaling functions. The transformation is carried out by designing a filter bank using coefficients to achieve perfect filter reconstruction of low pass and high pass filters. Due to the special choice of the mother wavelet, discrete wavelets are made orthogonal due to dilation and translations. Orthogonality is not an essential condition for the construction of the wavelet transform.
However, impose the condition of orthogonality selecting the wavelet allows us to obtain our bank filters from a single h(t) low-pass filter. The filter bank will consist of the filter low pass h(t) and a high-pass filter g(t). Two other reconstruction filters (h$\widehat{}$(t) and g$\widehat{}$(t)) for signal synthesis are obtained from the low-pass filters and high passes used for

signal analysis. The low-pass filter will provides the approximation of the signal and the high-pass filter will provide us with the details lost between approximations.

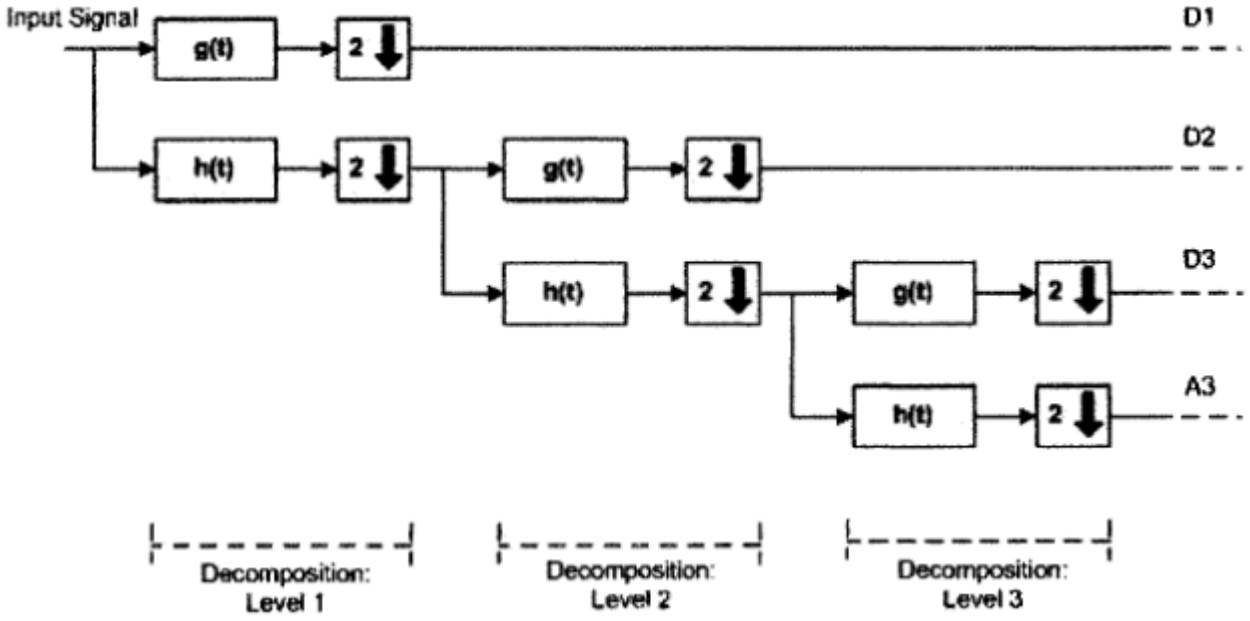


Figure 2.1: Transformation of discrete wavelets at several scales using a bank of wavelet filters, where An and Dn are the approximation and detail coefficients of the decomposition level n, signal decomposition/analysis,

From the wavelet transformation we can extract attributes of different types and at different levels of resolution. For the case of a 2D signal (image), the transformed in discrete wavelet is applied first row by row, then column by column [39] . Four images are then generated at each level as shown in the following figure:

Figure 2.2: example of decomposing the image on two levels,

## 2.3 Complex Wavelet Transform (CWT)

Complex Wavelets Transforms (CWT) is a relatively new improvement and a recent extension of the DWT. it has significant advantages over real wavelet transform for certain signal processing problems such as lack of shift invariance and lack of directional selectivity. CWT overcomes these problems:

**Shift invariance :**
Results from the downsampling operation at each level. When the input signal is shifted slightly, the amplitude of the wavelet coefficients at different levels varies dramatically. This can be problematic for operations that require shift invariance such as edge detection.

**Lack of directional selectivity :**
Discrete Wavelet Transform and we have seen that separable filtering along the rows and columns of an image produces four images at each level. The LH and HL bandpass subimages can select mainly horizontal or vertical edges, respectively, but the HH sub- image contains components from diagonal features of either orientation. This means it's 'poor directional selectivity'.
As DWT filters are real and separable, the frequency response is symmetric about zero in four quadrants of the 2D frequency space and therefore the DWT cannot distinguish between the two opposing diagonal directions.

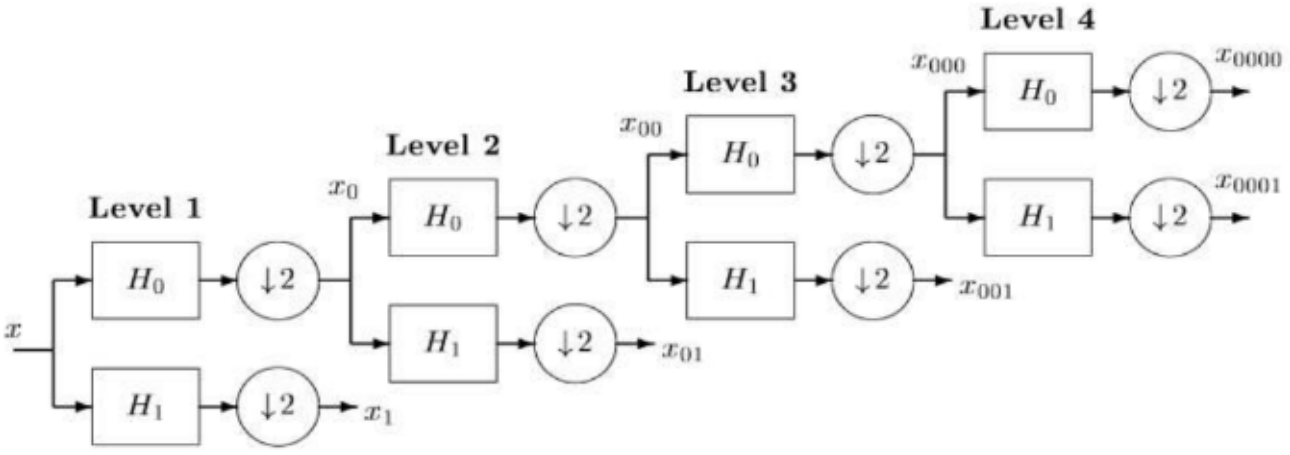


Figure 2.3: A filter tree showing the real wavelet decomposition , The wavelet filter H1 and the scaling function H0 are identical for all resolutions and have 0 phase

In order to avoid lack of shift invariance and directional selectivity, the filter output from each level requires being not downsampled [40], but it significantly increases the computational costs, Still it cannot distinguish between opposing diagonals because of separability of the transform. To distinguish the opposing diagonals with separable filters, the filter frequency responses are required to be asymmetric for positive and negative frequencies. With can be achieved using complex wavelets which suppresses negative frequency components, and leads to approximate shift invariance of CWT.

CWT with a wavelet transform can produce six directional sub-bands oriented at 75 ◦ ,15 ◦ , 45 ◦ , 75 ◦ , 15 ◦ , and 45 ◦ on a decomposition scale. By contrast, a wavelet transform only has three directional sub-bands oriented at 90 ◦ , 0 ◦ , and 45 ◦ on a scale.

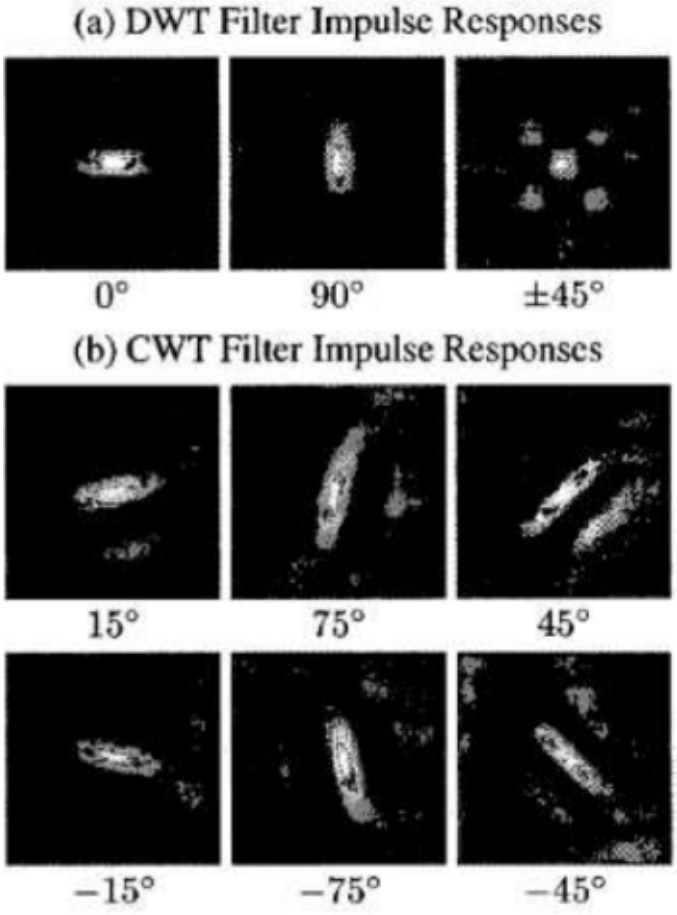


Figure 2.4: Filter impulse reponses in 2D (a) for the DWT and (b) for the CWT. the CWT has separate filters for + 45 ◦ and so can distinguish opposing diagonals.

This figure are presented four levels of the complex wavelet tree for a 1-D input signal x.

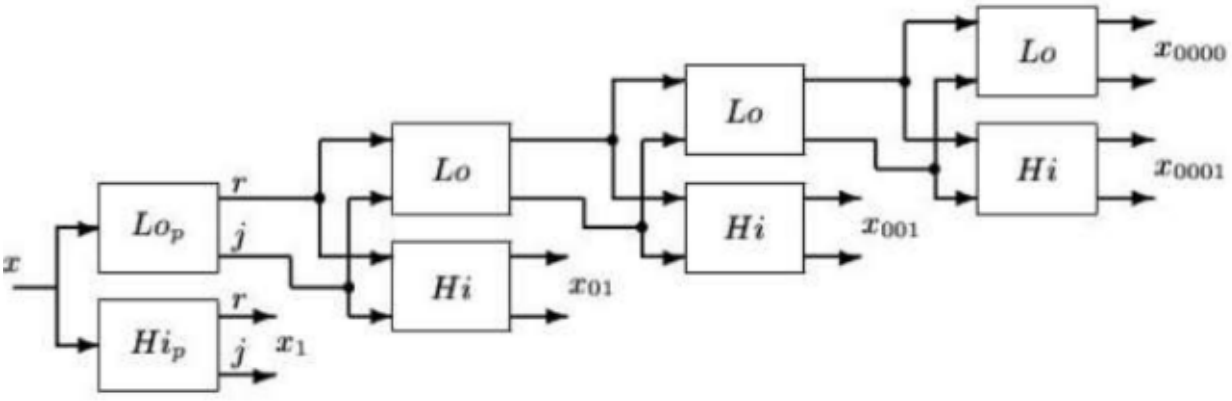


Figure 2.5: Four levels of Complex Wavelet Tree for real 1-D input signal x

The real and imaginary parts (r and j) of the inputs and outputs are shown separately. Where there is only one input to a block, it is a real signal.
The extension of complex wavelets to 2-D is achieved be separable filtering along rows and then columns, are presented two levels of the complex wavelet tree for a 2-D input image x, giving six directional bands at each level (the directions are shown for level 1). Components of 4-element 'complex' vectors are labeled r, j1, j2 and j1 j2.

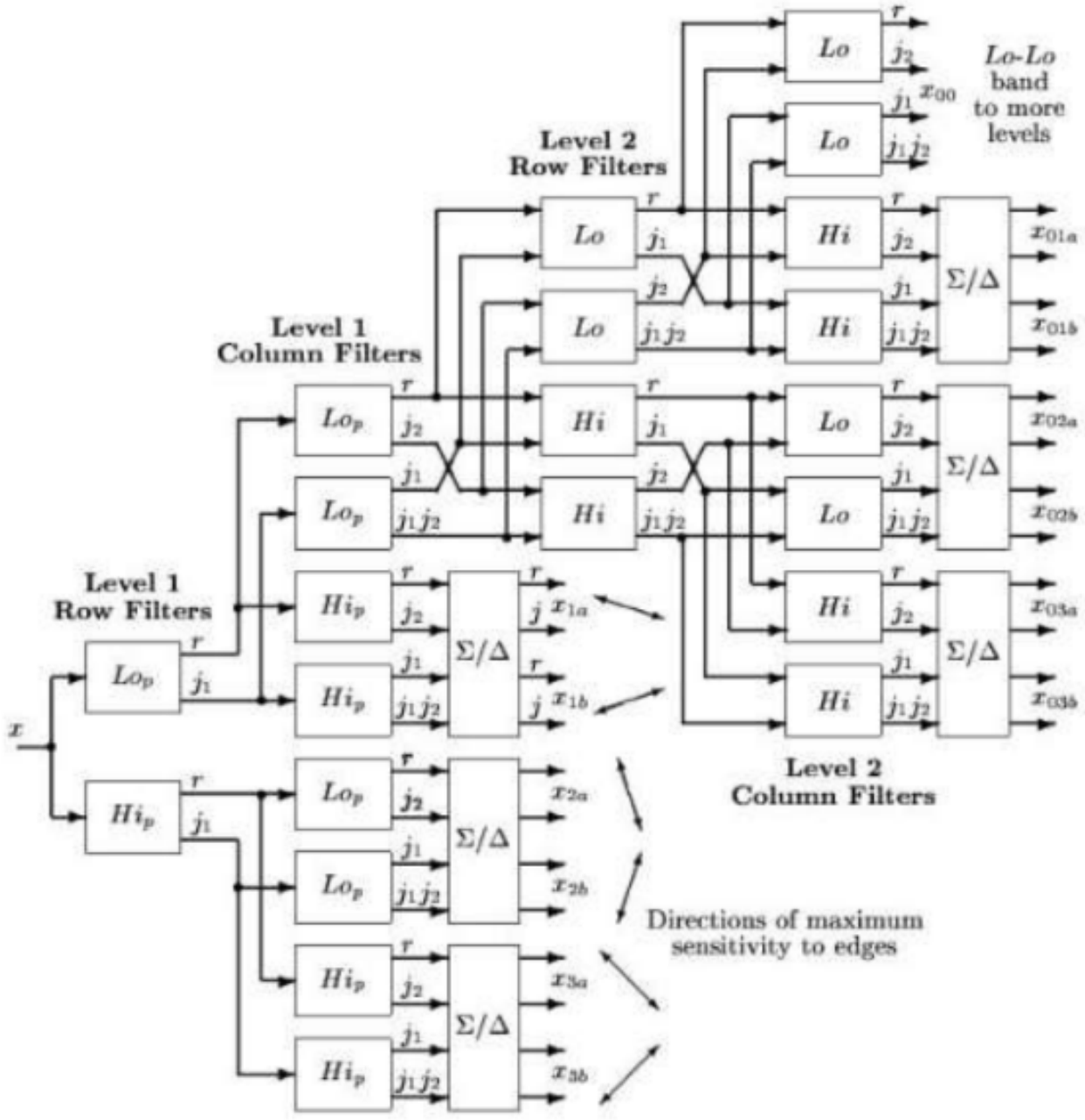


Figure 2.6: 2-D Complex wavelet tree

'Analytic filter' is the central to the design of all recent complex wavelet transforms complex-valued filtering that decomposes the real-complex signals into real and imaginary parts in transform domain. The real and imaginary coefficients are used to compute

amplitude and phase information, just the type of information needed to accurately describe the energy localization of oscillating functions (wavelet basis) [41].

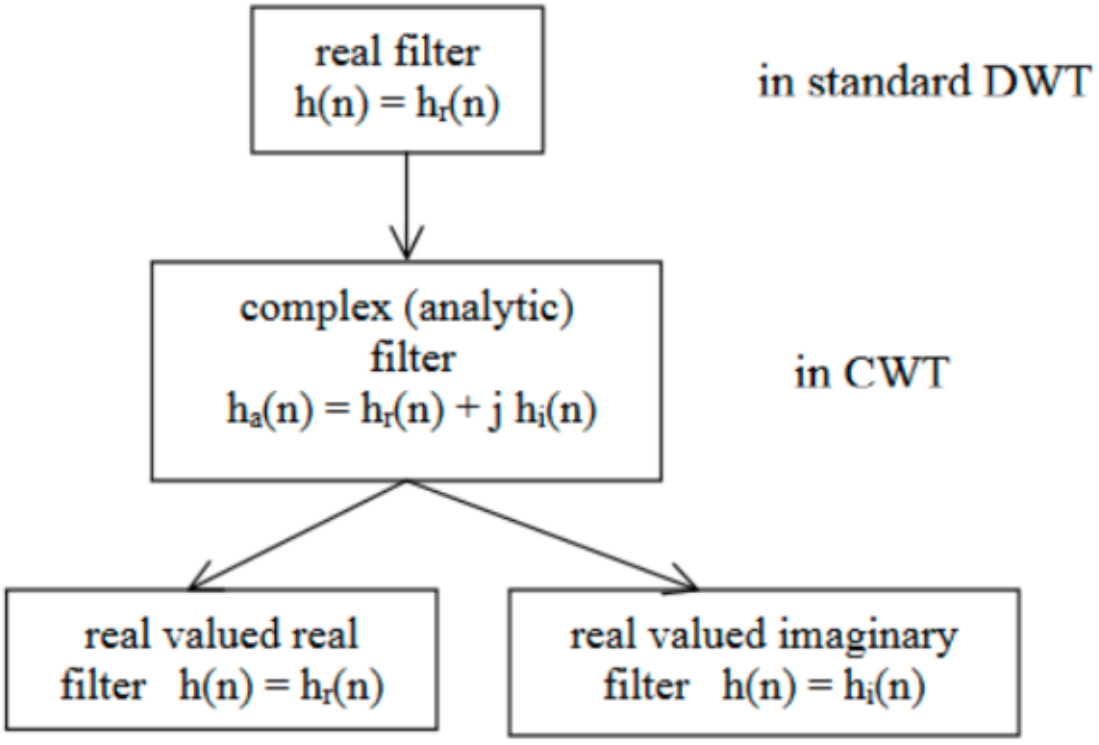


Figure 2.7: Interpretation of an analytic filter by 2-real filters

Its position within the support of the wavelet. The complex wavelet transform (CWT) employs analytic or quadrature wavelets guaranteeing magnitude phase representation, shift invariance and no aliasing
The development of CWTs follows, mainly, two directions. One direction regards the redundant transforms, meaning that if the input signal has N samples, then we will obtain M output coefficients, with M > N. From this class of transforms the most important are those relying on the dual-tree implementation. In this case, the original signal is passed through 2 real DWT filter-bank trees, the resulting coefficients being complex, having for real part the output values of the first tree and for imaginary part the output values of the second tree. From this type of transform we can mention Kingsbury's Dual-Tree Complex Wavelet Transform (DT CWT) [42] .

## 2.4 Advantages of CWT

1. Directional selectivity: Greatly complicates modeling and processing of geometric image features like ridges and edges, DWT does not have separate sub-bands for two opposing diagonal direction, while this is simply available in CWT.
2. Approximate shift invariance: Shift variance also complicates wavelet-domain processing, property of the CWT leads to get better robustness against applying the common attacks.

3. Better results in signal/image Denoising and Enhancement, bio- medical image analysis/registration.

## 2.5 Dual tree complex wavelet transform DT CWT

The dual tree complex wavelet transform (DT-CWT) is relatively a new wavelet transform, designed taking into account some defects of the DWT. The strong directional slectivity of DT-CWT comes from its ability to separate positive and negative frequencies in different bands. Similar to the adjustable filters, the DT-CWT is an over complete wavelet transform with limited redundancy of 2d, when d is the number of dimensions in the signal [43].
The DT-CWT is designed with two Daubechies wavelet bases. $\psi_h(t)$ and $\psi_g(t)$ must form a pair of Hilbert transforms $\psi_g(t) = (\psi_h(t))$, to overcome the problems of oscillation, aliasing, offset variance and lack of directionality associated with the TOP, as shown in [43] . The two wavelet bases are real and yield their own set of coefficient bands. However, it's considered as the real part of the transform, and $\psi_g(t)$ is treated as the imaginary part, which because the global basis is $\psi(t) = \psi_h(t) + j\psi_g(t)$ . Next Figure shows a representation of the DT-CWT filterbank.

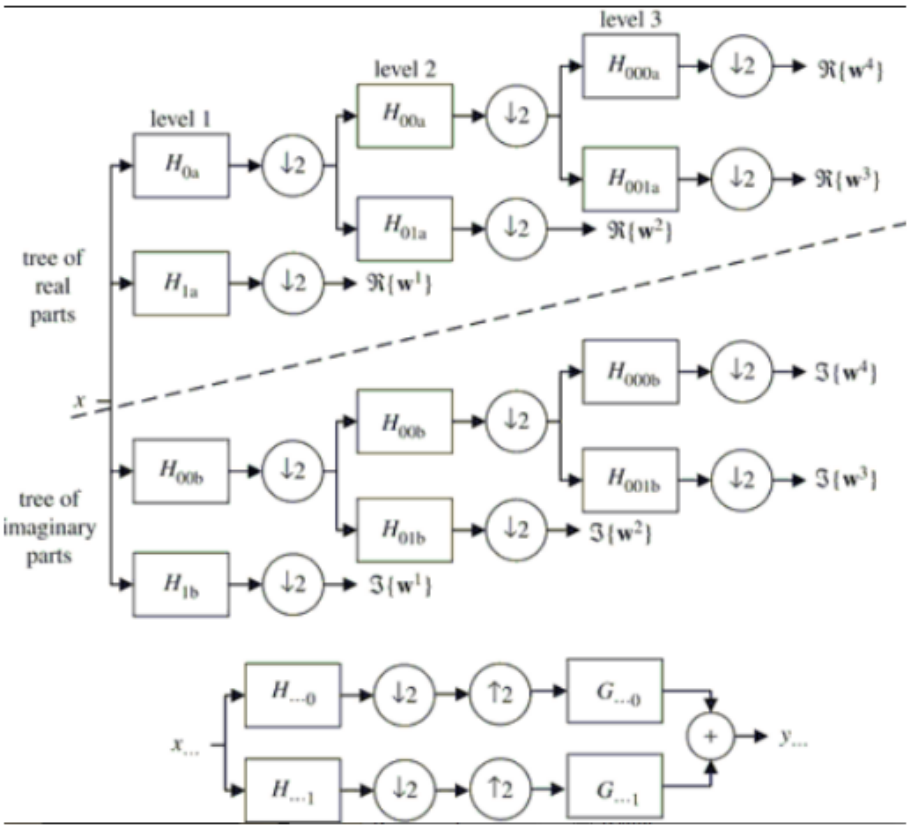


Figure 2.8: Representation of the dual tree of wavelet filters used by the DTCWT to compose a signal into real and imaginary parts of the wavelet coefficients complexes separately.

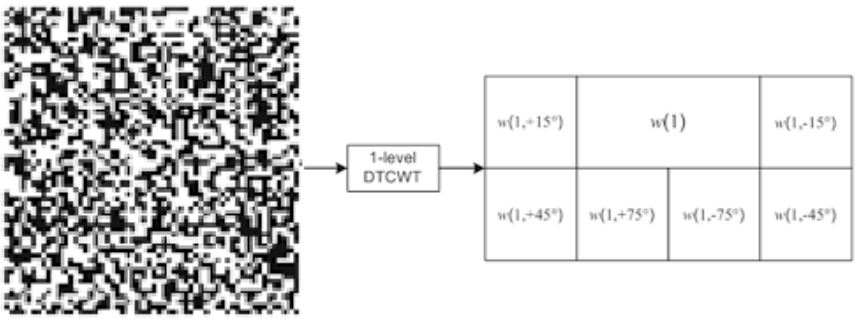


Figure 2.9: 1 Level DTCWT.

The use of a higher-dimensional DT-CWT may be more interesting than the use of a separable DWT of the same dimension. Indeed, the DT-CWT provides non-separable wavelets, by linearly combining different separable wavelets, all maintaining the simplicity of a separable transform.
The 2-D extension will be built by analyzing functions with a product vector of the functions 1D. the three base row-column wavelets (LH,HL,HH):
$\Psi_1(x,y) = \varphi(x)\Psi(y)$
$\Psi_2(x,y) = \Psi(x)\varphi(y)$
$\Psi_3(x,y) = \Psi(x)\Psi(y)$
We use wavelet complex $\Psi(t) = \Psi_h(t) + j\Psi_g(t)$ and HH wavelet:

$$\psi(x,y) = \psi(x)\psi(y) = [\psi_h(x) + j\psi_g(x)][\psi_h(x) + j\psi_g(y)] \tag{2.5}$$

$$= \psi_h(x)\psi_h(y) - \psi_g(x)\psi_g(y) + j[\psi_g(x)\psi_h(y) + \psi_h(x)\psi_g(y)] \tag{2.6}$$

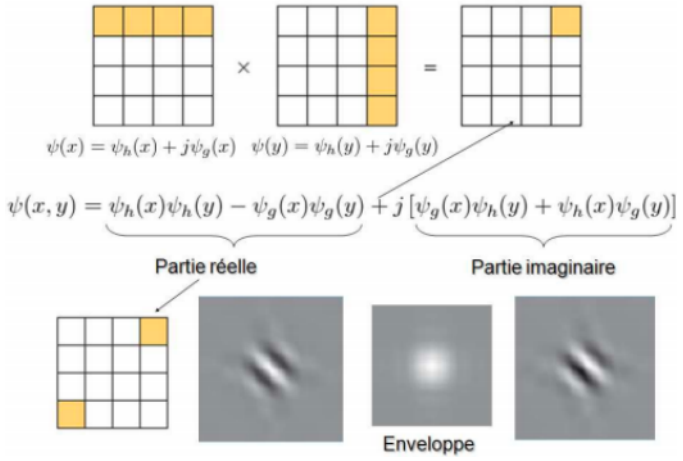


Figure 2.10: Transformed into complex 2-D wavelets and associated frequency cutting

The real part of this wavelet has a symmetric spectrum capturing only one diagonal direction, if we want another direction we can set up a another combination as shown in

the following figure:

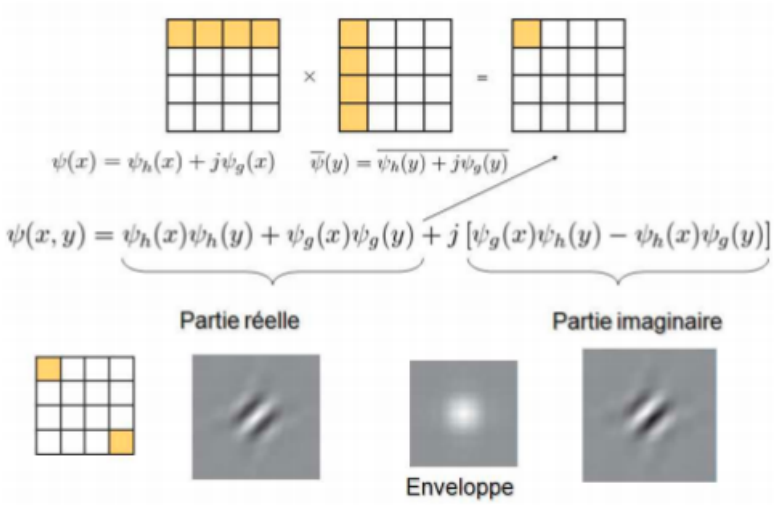


Figure 2.11: 2nd Complex wavelet transform 2-D and associated frequency cutting

Here are the other wavelet and the associated frequency windows in the following matrix:

$$\begin{bmatrix} \psi(x)\psi(y); \psi(x)\overline{\psi}(y) \\ \phi(x)\psi(y); \phi(x)\overline{\psi}(y) \\ \psi(x)\phi(y); \psi(x)\overline{\phi}(y) \end{bmatrix}$$

### 2.5.1 Filter design for DT-CWT

As in the case of the filters design for real wavelet transform, there are different approaches to designing filters for the DT-CWT. In the following we describe methods to build filters satisfying the properties the following desired:
- Delay property of an approximate sub-sampling
- PR (orthogonal or biorthogonal)
- Finished media (FIR filters)
- Moments of disappearance/good stopband
- Linear phase filters (desired, but not required of a wavelet transform so that it is approximately analytical).

An approach to designing dual-tree filters is to let $h_0(n)$ be an existing wavelet filter. Then, given $h_0(n)$, we must design $g_0(n)$ in such a way as to simultaneously satisfy $g_0(e^i) \approx (e^{-j0.5w})H_0(e^{iw})$ and the Conditions. Unfortunately, this results sometimes in g0(n) being significantly longer than h0(n). Grace at the joint design of h0(n) and g0(n), a pair of filters of equal length is obtained (or almost equal), where both are relatively short. It should be noted, however, that Filters for the dual-tree CWT are usually a little longer than the real wavelets filters with a similar number of moments of disappearance, due to the additional constraints that the filters must approximately satisfy. In the following, we describe three methods of dual-tree filter design.

#### 2.5.1.1 Linear-Phase Biorthonal Solution

The first solution, introduced in [44], defines h0(n) as a symmetric finite support filter (FIR) of odd length (type I) and defines $g_0(n)$ as a symmetrical FIR filter of even length (type II), so that for odd N

$$h(n) = h_0(N-1-n) \tag{2.7}$$

$$g(n) = g_0(N-1-n) \tag{2.8}$$

This solution must be a biorthogonal solution (the filters of the FB synthesis are not not time-reversed versions of FB scan filters). This is due to the fact that two-channel BFs of the actual orthonormed FIR cannot be symmetrical (except for Haar's solution). Therefore, $h_0(n)$ and $g_0(n)$ must be designed in such a way as to satisfy approximately the magnitude condition. Therefore, $h_0(n)$ and $g_0(n)$ must be designed to satisfy approximately the magnitude condition.

#### 2.5.1.2 Solution q-SHIFT

The second solution, introduced in [45]:

$$g_0(n) = h_0(N-1-n) \tag{2.9}$$

Where N, now even, is the length of $h_0(n)$, which is supported over 0 n N1. In this case, the magnitude part (10) of the delayed half-sample condition is exactly satisfied due to the inverse relationship between the filters, but the phase part, is not accurate. Therefore, $h_0(n)$ and $g_0(n)$ should be designed to satisfy approximately at the magnitude condition.

#### 2.5.1.3 Common Factor Solution

The third solution, introduced in [46], can be used to design orthonormal and biorthogonal solutions for dual-tree CWT.
In this approach

$$h_0(n) = f(n) \times d(n) \tag{2.10}$$

$$g_0(n) = f(n) \times d(L-n) \tag{2.11}$$

Where $\times$ represents the convolution in discrete time and where d(n) is supported on $0 \leq n \leq L$.
As for the q-shift solution, for solutions of this type, the magnitude part of the delayed

condition of the half sample is exactly satisfied, but the phase part is not. Filters must be designed so that the phase condition is approximately satisfied.

The core idea behind DT-CWT is the use of complexe valued scaling and wavelet functions in Eqs.

$$\phi(t) = \phi^1(t) + i\phi^2(t), \psi(t) = \psi^1(t) + i\psi^2(t) \tag{2.12}$$

Where $\phi^1$ and $\psi^1$ are real parts and even functions where as $\phi^2$ and $\psi^2$ are imaginary parts and odd functions. The two real and imaginary parts are selected in such a way that they form a Hilbert transform pair, i.e.,

$$\phi^1(t) = H[\phi^2(t)], \psi^1(t) = H[\psi^2(t)] \tag{2.13}$$

Where $H$ is the hilbert transform operator, Using the concept of a complex wavelet, the complex wavelet transform is given as

$$f(t) = \sum_{n=-\infty}^{\infty} C^c_{j_0,n}(\phi^1_{j_0}(t-n) + i\phi^2_{j_0}(t-n))$$
$$+ \sum_{j=j_0}^{\infty} \sum_{n=-\infty}^{\infty} D^c_{j,n}(\psi^1_j(t-n) + i\psi^2_j(t-n)) \tag{2.14}$$

Where $C^c_{j_0,n}$ and $D^c_{j,n}$ Are the scaling and wavelet coefficients associated with complex wavelet transform and are given as :

$$C^c_{j_0,n} = \langle fK_a, \phi_{j_0}\rangle = \int_{-\infty}^{\infty}\int_{-\infty}^{\infty} f(t)K_a(t,x)$$
$$\times(\phi^1_{j_0}(t-n) + i\phi^2_{j_0}(t-n))dtdx = C^1_{j_0,n} + iC^2_{j_0,n} \tag{2.15}$$

$$D^c_{j_0,n} = \langle fK_a, \psi_j\rangle = \int_{-\infty}^{\infty}\int_{-\infty}^{\infty} f(t)K_a(t,x)$$
$$\times(\psi^1_j(t-n) + i\psi^2_j(t-n))dtdx = D^1_{j,n} + iD^2_{j,n} \tag{2.16}$$

Using Eq (3.15) and (3.16), Eq (3.14) becomes

$$f(t) = \sum_{n=-\infty}^{\infty} (C^1_{j_0,n} + iC^2_{j_0,n})(\phi^1_{j_0}(t-n) + i\phi^2_{j_0}(t-n))$$
$$+ \sum_{j=j_0}^{\infty} \sum_{n=-\infty}^{\infty} (D^1_{j,n} + iD^2_{j,n})(\psi^1_j(t-n) + i\psi^2_j(t-n)) \tag{2.17}$$

The above equation can be rearranged as :

$$f(t) = \sum_{n=-\infty}^{\infty} C^1_{j_0,n}(\phi^1_{j_0}(t-n) + i\phi^2_{j_0}(t-n))$$
$$+ \text{i} \sum_{n=-\infty}^{\infty} C^2_{j_0,n}(\phi^1_{j_0}(t-n) + i\phi^2_{j_0}(t-n))$$

$$+ \sum_{j=j_0}^{\infty} \sum_{n=-\infty}^{\infty} D_{j,n}^{1}(\psi_j^1(t-n) + i\psi_j^2(t-n))$$

$$+ \text{i} \sum_{j=j_0}^{\infty} \sum_{n=-\infty}^{\infty} D_{j,n}^{2}(\psi_j^1(t-n) + i\psi_j^2(t-n)) \quad (2.18)$$

Seperating the real and imaginary parts in Eq, we get

$$f(t) = (\sum_{n=-\infty}^{\infty} C_{j_0,n}^{1}(\phi_{j_0}^1(t-n) + i\phi_{j_0}^2(t-n))$$

$$+ \sum_{j=j_0}^{\infty} \sum_{n=-\infty}^{\infty} D_{j,n}^{1}(\psi_j^1(t-n) + i\psi_j^2(t-n)))$$

$$+ \text{i}(\sum_{n=-\infty}^{\infty} C_{j_0,n}^{2}(\phi_{j_0}^1(t-n) + i\phi_{j_0}^2(t-n))$$

$$+ \sum_{j=j_0}^{\infty} \sum_{n=-\infty}^{\infty} D_{j,n}^{2}(\psi_j^1(t-n) + i\psi_j^2(t-n))) \quad (2.19)$$

From the above equation, it is clear that two wavelet tree structures are obtained using complex values scaling and wavelet functions .

## 2.6 Singular Value Decomposition SVD

### 2.6.1 Introduction

Singular value decomposition is a linear algebra technique that decomposes a given matrix into three component matrices [47]:
(1) Left singular vectors;
(2) Set of singular values (diagonal entries);
(3) Right singular vectors.
These two matrices consist of singular vectors that provide information about the structure of the original matrix. Singular values describe the strength of a given component of the original matrix. The SVD theorem [48] states that, given a matrix M, there is a decomposition of M such that A = USV
The SVD of a matrix can also be described geometrically. SVD shows that the value of any matrix A can be reconstructed by rotating (U) and then increasing the Matrix values (S) followed by another rotation (V) [49]

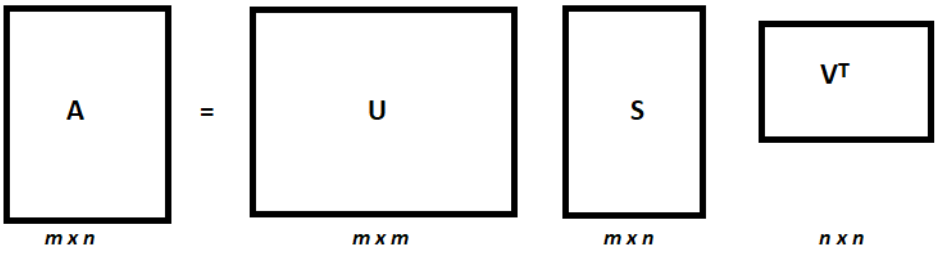


Figure 2.12: llustration of Factoring A to USV

For instance, if A represents the coordinates that produce a 3D shape,then the shape can be constructed from the rotation information in U and V,along with stretching the shape out to its proper size with the information in S [49] This type of decomposition is important and useful because the rotation matrix separates the key components of the original matrix and finds relationships between data points, while the strength matrix indicates which of the key components highlighted in the rotational matrices are the most important [47] [49] [50]. The core idea of the study is to separate the key components of the original matrix, which is the basis for using SVD. If the matrix consists of change logs, defect information, or other data from the development process, these key components highlight the underlying structure in the codebase. SVD has other uses in data processing. For example, this technique can be used for image and signal compression. A grayscale image can be represented as a two-dimensional matrix of intensity values, indicating how dark a particular pixel is. In this case, we can treat the image matrix itself as the original M matrix and perform SVD on it. when the decomposition is completed, the resulting matrices, USV, can also be represented as the sum of component matrices, as shown in Equation

$$M = U_1 S_{1,1} V_1 + U_2 S_{2,2} V_2 + ..... + U_K S_{K,K} V_K \tag{2.20}$$

Where k is less than or equal to the rank of the matrix. This provides a rank k approximation of the matrix. The first component of this factorization gives the component that has the largest single value and contributes the most variability to the overall matrix. As subsequent components are assembled, the matrix, as well as the image itself, begins to return to its original form [47] [50].

### 2.6.2 Definition of the SVD [Liu and Tan, 2002]

Any matrix A, of size m × n, can be decomposed into a product of three matrices as follows:

$$A = USV^T = \sum_{i=1}^{r} \lambda_i U_i V_i^T. \tag{2.21}$$

Where U and V are orthogonal matrices, respectively of dimensions m × m and n × n. We have : $U^T U = I$ and $V^T V = I$
S is a diagonal matrix of size n×n composed of the singular values $\lambda_i$ in order decreasing, on the diagonal and T is the transposition operator. We can also write:
$S = diag(\lambda_1, \lambda_2, ..., \lambda_r)$ such that $\lambda_1 \geq \lambda_2 \geq ... \geq \lambda_r > 0$ where r = min(m,n) the rank of the matrix A is equal to the number of non-zero singular values (SVs) that the matrix A [51].

### 2.6.3 SVD Watermarking

SVD watermarks are designed to work with binary files, For an image of $N \times N$ pixels and a binary watermark of $P \times P$ pixels, divided the image into $(N/4) \times (N/4)$ non overlapping blocks whose size is $4 \times 4$ pixels [52]. which is based to deicide the positions of embedded blocks for each watermark bit. The watermarking embedding procedure show in this figure

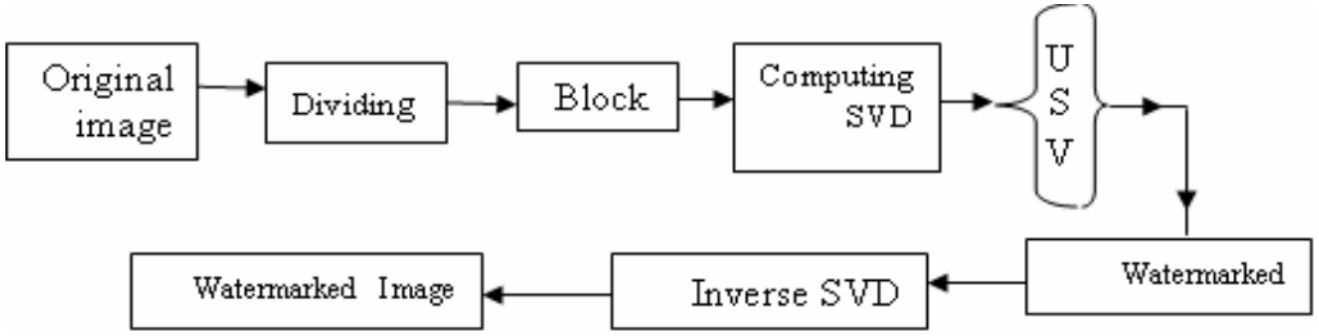


Figure 2.13: Watermark embedding procedure

Using SVD on different blocks of the image, for each generated Sj matrix of each block Bj, where $1 \leq j \leq (N/4) \times (N/4)$ , as below, they let s3 be equal to s2 ans set s2 be equal to $s2 + \alpha \times wi$ for embedding the binary value of the watermark, where $\alpha$ is a constant and $wi$ is the watermark bit, Each Sj matrix of block Bj contains the value of the watermark. After embedding the watermark into the sj matrix of block Bj, the embedded block Bj is obtained by inverting its corresponding U, V [52].
The proposed watermarking can be divided into two methods: embedding ; and extraction and restoration [53].

### 2.6.4 Properties of the SVD

SVD has many properties ,here are some of them [53]:
- The singular value $\alpha_1, \alpha_2, \alpha_n$ are unique, however , the matrices U and V are not unique.
- Since $A^T A = V S^T S V^T$, So V diagonalizes $A^T A$, it follows that the $V_j$ are the eigenvector of $A^T A$.
- Since $AA^T = USS^T U^T$, so it followes that U diagonalizes $AA^T$ and that the $U_i$ are the eigenvectors of $AA^T$
- If A has rank of r then $v_i, v_j, ..., v_r$ form an orthonormal basis for range space of $A^T, R(A^T), and u_i, u_j, ..., u_i$ form and orthonormal basis for . range space A,R(A)
- The rank of matrix A is equal to the number of its nonzero singular values [54].

### 2.6.5 Advantages of SVD

- Robust against JPEG compression, Gaussian noise, sharpening, and cropping [55]
- Preserves image quality [55]
- Solves false positive detection problem [55]
- Better robustness and imperceptibility [55]
- Great energy compaction and low computation cost compared to other transform domain techniques [56]

## 2.7 Conclusion

The second chapter presented the Complex wavelet transform which is a new improved method of the wavelet transform, We presented the mathematical background of this method, and the advantages gained by the CWT. It also presented the implemented method Dual Tree Complex wavelet transform which is its recent enhanced design of the CWT, We demonstrated in detail the DTCWT mathematical components and equations like the filterbanks and its different implementations (Linear-Phase Biorthonal Solution, Solution q-SHIFT and Common Factor Solution).
The chapter also introduced the concept of Singular Value decomposition, Its utilization in matrices and watermarking, And finishes with the properties of SVD and the advantages it offers in addition to the CWT advantages on the watermarking process.
The importance of using the dual tree complex wavelet transform along with the singular value decomposition is reducing the window of operation of the subband (using the diagonal entries of the subband) when inserting the watermark
In the next chapter, we will show the experimental part of our work which both combines Dual-Tree Complex Wavelet Transform and Singular Value Decomposition to gain the advantages they offer in the watermarking field and we discuss the different results obtained.

# CHAPTER 3

# IMPLEMENTATION AND RESULTS.

## 3.1 Introduction

In the previous chapters, we have studied the different watermarking techniques used for medical images.
In this chapter, we propose an effective and robust watermarking method applied to medical imaging, which is the one that combines DTCWT and SVD watermarking techniques. The watermarked image quality is measured with well-known metrics used in image processing such as the PSNR, SSIM and MSE. The experimental results show the watermark robustness against several geometric and signal processing distortions.

## 3.2 Material resources

| - | PC 1 | PC 2 |
|---|---|---|
| Model | DELL | Lenovo |
| CPU | Intel(R)i5-2520M 2.5GHz | Intel(R)i5-5200U 2.20GHz |
| Graphic card | Intel(R)HD graphique 3000 | Intel(R)HD graphique 5500 |
| RAM | 4 GB | 8 GB |
| Hard disk | 500 GB | 500 GB |
| OS | Windows 10 PRO | Windows 10 PRO |

Table 3.1: Material resources

## 3.3 MATLAB

### 3.3.1 Introduction

MATLAB is a programming platform designed specifically for engineers and scientists to analyze and design systems and products that transform our world. The heart of MATLAB is the MATLAB language, a matrix-based language allowing the most natural

expression of computational mathematics [57].


Figure 3.1: MATLAB logo

### 3.3.2 Origins

MATLAB was invented by mathematician and computer programmer Cleve Moler. [58] The idea for MATLAB was based on his 1960s PhD thesis. [58] Moler became a math professor at the University of New Mexico and started developing MATLAB for his students [58] as a hobby. [59] He developed MATLAB's initial linear algebra programming in 1967 with his one-time thesis advisor, George Forsythe. [58] This was followed by Fortran code for linear equations in 1971. [58]

In the beginning (before version 1.0) MATLAB "was not a programming language; it was a simple interactive matrix calculator. There were no programs, no toolboxes, no graphics. And no ODEs or FFTs."

The first early version of MATLAB was completed in the late 1970s. [58] The software was disclosed to the public for the first time in February 1979 at the Naval Postgraduate School in California. [59] Early versions of MATLAB were simple matrix calculators with 71 pre-built functions. [60] At the time, MATLAB was distributed for free [61] [62] to universities. [63] Moler would leave copies at universities he visited and the software developed a strong following in the math departments of university campuses. [64]

In the 1980s, Cleve Moler met John N. Little. They decided to reprogram MATLAB in C and market it for the IBM desktops that were replacing mainframe computers at the time. [58] John Little and programmer Steve Bangert re-programmed MATLAB in C, created the MATLAB programming language, and developed features for toolboxes. [59]

### 3.3.3 Commercial development

MATLAB was first released as a commercial product in 1984 at the Automatic Control Conference in Las Vegas. [58] [59] MathWorks, Inc. was founded to develop the software [62] and the MATLAB programming language was released. [61] The first MATLAB sale was the following year, when Nick Trefethen from the Massachusetts Institute of Technology bought ten copies. [59] [65]

By the end of the 1980s, several hundred copies of MATLAB had been sold to universities for student use. [59] The software was popularized largely thanks to toolboxes created by experts in various fields for performing specialized mathematical tasks. [61] Many of

the toolboxes were developed as a result of Stanford students that used MATLAB in academia, then brought the software with them to the private sector. [59]

Over time, MATLAB was re-written for early operating systems created by Digital Equipment Corporation, VAX, Sun Microsystems, and for Unix PCs. [59] [60] Version 3 was released in 1987.[33] The first MATLAB compiler was developed by Stephen C. Johnson in the 1990s. [60]

In 2000, MathWorks added a Fortran-based library for linear algebra in MATLAB 6, replacing the software's original LINPACK and EISPACK subroutines that were in C. [60] MATLAB's Parallel Computing Toolbox was released at the 2004 Supercomputing Conference and support for graphics processing units (GPUs) was added to it in 2010. [60]

### 3.3.4 Release history

| Version [66] | Release name | Year | Version | Release name | Year |
|---|---|---|---|---|---|
| MATLAB 1.0 | | 1984 | MATLAB 2 | | 1986 |
| MATLAB 3 | | 1987 | MATLAB 3.5 | | 1990 |
| MATLAB 4 | | 1992 | MATLAB 4.2c | | 1994 |
| MATLAB 5.0 | Volume 8 | 1996 | MATLAB 5.1 | Volume 9 | 1997 |
| MATLAB 5.1.1 | R9.1 | 1997 | MATLAB 5.2 | R10 | 1998 |
| MATLAB 5.2.1 | R10.1 | 1998 | MATLAB 5.3 | R11 | 1999 |
| MATLAB 5.3.1 | R11.1 | 1999 | MATLAB 6.0 | R12 | 2000 |
| MATLAB 6.1 | R12.1 | 2001 | MATLAB 6.5 | R13 | 2002 |
| MATLAB 6.5.1 | R13SP1 | 2003 | MATLAB 6.5.2 | R13SP2 | 2003 |
| MATLAB 7 | R14 | 2004 | MATLAB 7.0.1 | R14SP1 | 2004 |
| MATLAB 7.0.4 | R14SP2 | 2005 | MATLAB 7.1 | R14SP3 | 2005 |
| MATLAB 7.2 | R2006a | 2006 | MATLAB 7.3 | R2006b | 2006 |
| MATLAB 7.4 | R2007a | 2007 | MATLAB 7.5 | R2007b | 2007 |
| MATLAB 7.6 | R2008a | 2008 | MATLAB 7.7 | R2008b | 2008 |
| MATLAB 7.8 | R2009a | 2009 | MATLAB 7.9 | R2009b | 2009 |
| MATLAB 7.9.1 | R2009bSP1 | 2010 | MATLAB 7.10 | R2010a | 2010 |
| MATLAB 7.11 | R2010b | 2010 | MATLAB 7.11.1 | R2010bSP1 | 2011 |
| MATLAB 7.11.2 | R2010bSP2 | 2011 | MATLAB 7.12 | R2011a | 2011 |
| MATLAB 7.13 | R2011b | 2011 | MATLAB 7.14 | R2012a | 2012 |
| MATLAB 8 | R2012b | 2012 | MATLAB 8.1 | R2013a | 2013 |
| MATLAB 8.2 | R2013b | 2013 | MATLAB 8.3 | R2014a | 2014 |
| MATLAB 8.4 | R2014b | 2014 | MATLAB 8.5 | R2015a | 2015 |
| MATLAB 8.5 | R2015aSP1 | 2015 | MATLAB 8.6 | R2015b | 2015 |
| MATLAB 9.0 | R2016a | 2016 | MATLAB 9.1 | R2016b | 2016 |
| MATLAB 9.2 | R2017a | 2017 | MATLAB 9.3 | R2017b | 2017 |
| MATLAB 9.4 | R2018a | 2018 | MATLAB 9.5 | R2018b | 2018 |
| MATLAB 9.6 | R2019a | 2019 | MATLAB 9.7 | R2019b | 2019 |
| MATLAB 9.8 | R2020a | 2020 | MATLAB 9.9 | R2020b | 2020 |
| MATLAB 9.10 | R2021a | 2021 | MATLAB 9.11 | R2021b | 2021 |
| MATLAB 9.12.0 | R2022a | 2022 | | | |

Table 3.2: MATLAB version

## 3.4 EXPERIMENTAL RESULTS

In the performed experiment, a knee MRI image has been selected as the host image (Figure 3.2), for the watermark a small 33x33 image has been selected as the watermark image (Figure 3.3).


Figure 3.2: Host image

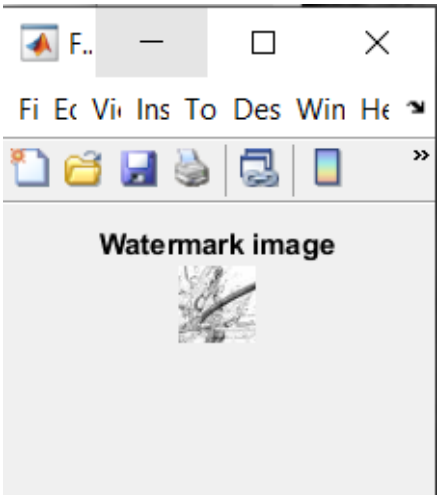


Figure 3.3: Watermark image

## 3.4.1 Evaluation metrics

### 3.4.1.1 MSE

Mean Squared Error is a model evaluation metric often used with regression models. The mean squared error of a model with respect to a test set is the mean of the squared prediction errors over all instances in the test set. The prediction error is the difference between the true value and the predicted value for an instance. [67]
A closer MSE value to 0, means better result.

### 3.4.1.2 PSNR

Peak signal-to-noise ratio (PSNR) is an engineering term for the ratio between the maximum possible power of a signal and the power of corrupting noise that affects the fidelity of its representation. Because many signals have a very wide dynamic range, PSNR is usually expressed as a logarithmic quantity using the decibel scale..
Higher PSNR value means a better result.

### 3.4.1.3 SSIM

The structural similarity index measure (SSIM) is a method for predicting the perceived quality of digital television and cinematic pictures, as well as other kinds of digital images and videos. SSIM is used for measuring the similarity between two images. The SSIM index is a full reference metric; in other words, the measurement or prediction of image quality is based on an initial uncompressed or distortion-free image as reference.
A closer SSIM value to 1, means better result.

The evaluation metrics (MSE, PSNR, SSIM) fonctions used are pre-defined by matlab

## 3.4.2 Embedding process

We suggest the following steps of the embedding phase method and the related diagram is shown in figure (3.4).
(i) Consider a host image (Figure 3.2)
(ii) The Complex Wavelet Transform of the host image is calculated according to the selected decomposition level (first level).
(iii) To select the more suitable sub-bands, to embed the SVs of the watermark, both robustness against the attacks and the best quality of the watermarked image should be considered.
Choosing the first sub-band causes less quality fidelity. To choose the appropriate sub-bands for embedding watermark, each subband is tested.
(iv) Combine SVs of the watermark with the SVs of the selected sub-bands using appropriate scaling factor (a), as illustrated in Equation :
$newval = (a * SVwatermark) + SVhost$
in which : -SV watermark are values of the watermark after applying SVD
-SV host are values of the selected subband after applying SVD
(v) Using ICWT, the watermarked image will be constructed.

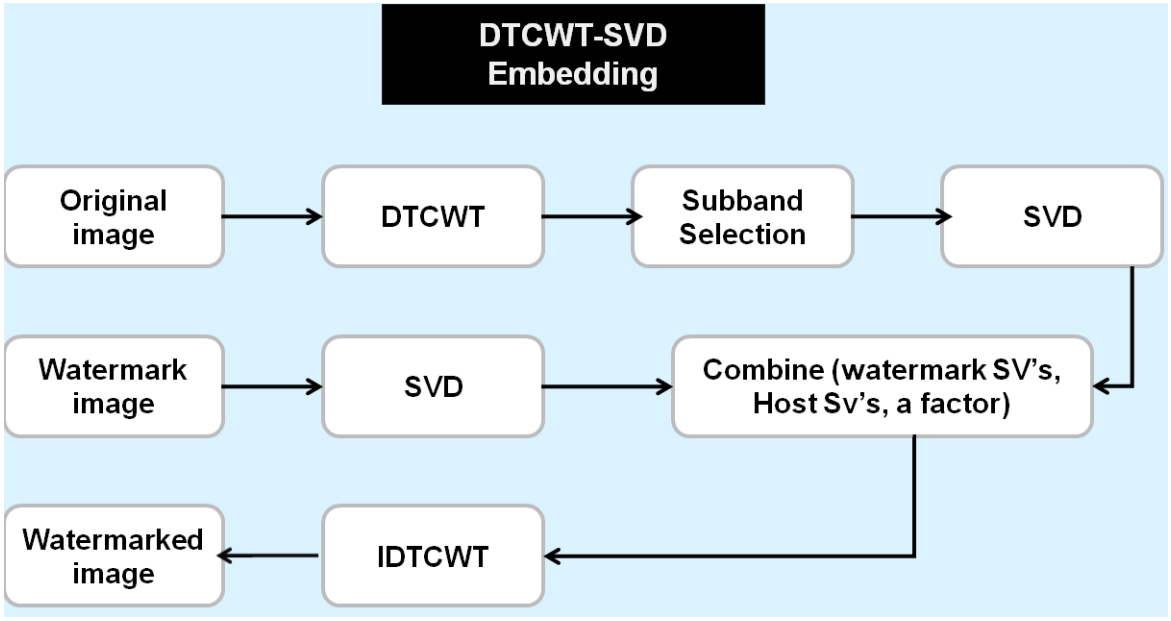


Figure 3.4: DTCWT-SVD Embedding


Figure 3.5: Watermarked image

### 3.4.3 Extraction process

We suggest the following steps of the extraction phase method and the related diagram is shown in figure (3.6).
(i) Calculate the complex wavelet transform of the watermarked image (Figure 3.5) to the decomposition level (first level), consider the appropriate sub-bands, and compute the corresponding SVs.

(ii) Compute the SVs of the mentioned sub-band applying SVD.
(iii) Obtain the SVs of watermark through Equation :
$newval = SVwatermarked/a$
in which : SV watermarked are the singular values of the watermarked image a is the scale factor
(iv) Inverse singular value decomposition is applied, to extract the watermark.

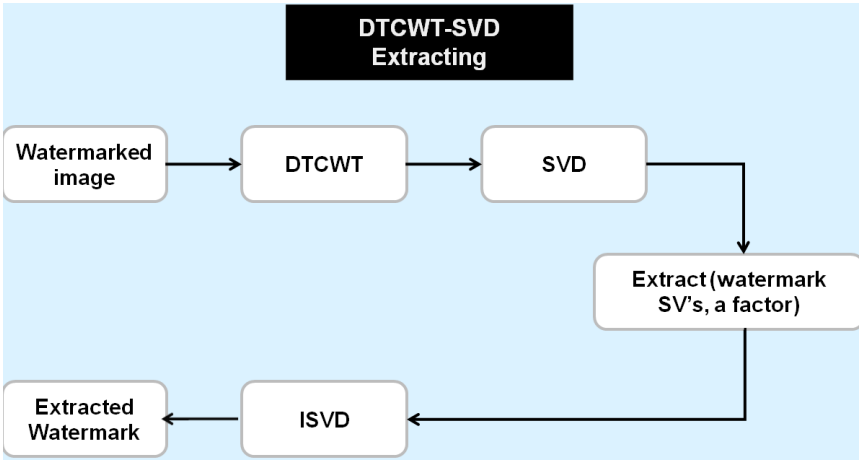


Figure 3.6: DTCWT-SVD Extracting

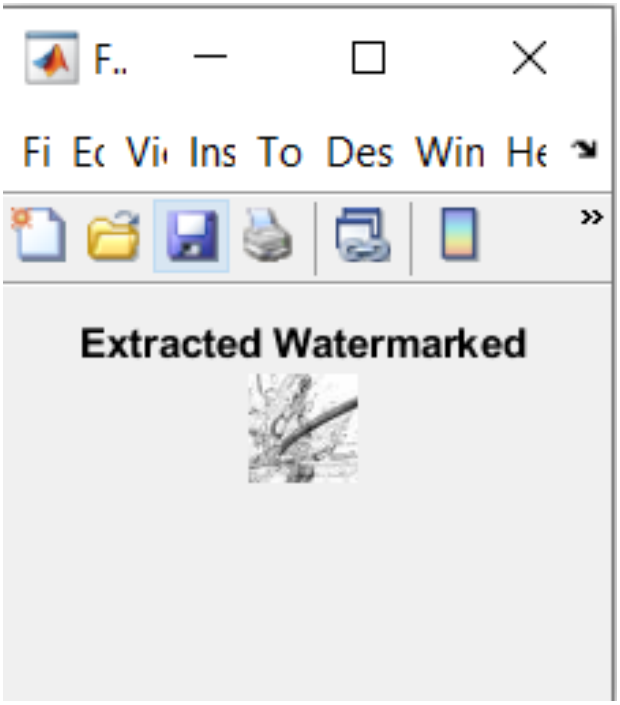


Figure 3.7: Extracted watermarked

### 3.4.4 Level and subband selection tests

#### 3.4.4.1 Level Selection tests

The most commonly implemented Decomposition levels in wavelet transforms (level 1, level 2, level 3) were tested to select the most suitable Level for watermarking process.

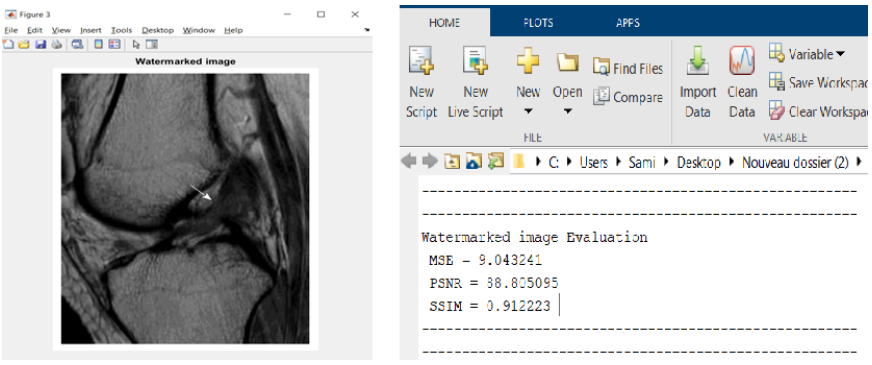


Figure 3.8: First Level

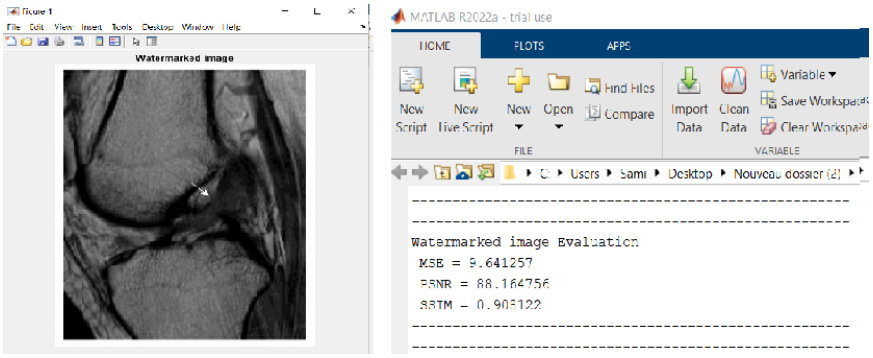


Figure 3.9: Second Level

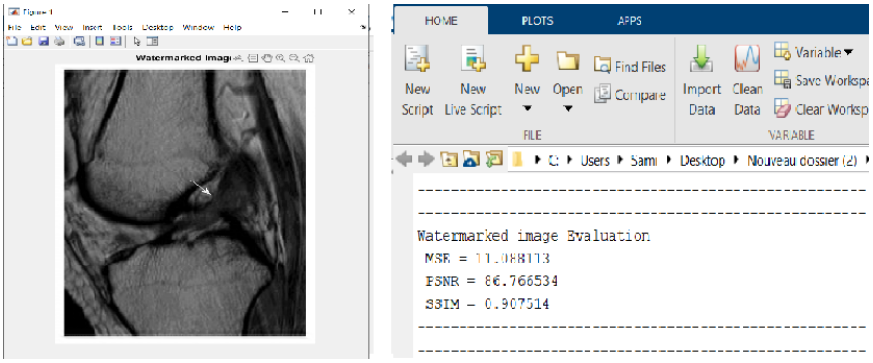


Figure 3.10: Third Level

According to the obtained results Level 1 is selected, Level 1 gives the best results considering the evaluation results and computational time. Level 3 gives better evaluation results (PSNR, MSE, SSIM) than Level 2 although it's a small difference, where there is no visual difference between the result images, another drawbacks of Level 2 and 3 is that it takes more computational time .

#### 3.4.4.2 Subband Selection tests

We tested the obtained subbands using the evaluation metrics (PSNR, MSE, SSIM), in aim to select the most suitable for the watermarking process out of the six subbands.

```
--------------------------------------------------------
--------------------------------------------------------
Watermarked image Evaluation
 MSE = 10.827428
 PSNR = 87.004446
 SSIM = 0.888796
--------------------------------------------------------
--------------------------------------------------------
```

Figure 3.11: Subband 1

```
--------------------------------------------------------
--------------------------------------------------------
Watermarked image Evaluation
 MSE = 8.670071
 PSNR = 89.226502
 SSIM = 0.912177
--------------------------------------------------------
--------------------------------------------------------
```

Figure 3.12: Subband 2

```
--------------------------------------------------------
--------------------------------------------------------
Watermarked image Evaluation
 MSE = 11.656208
 PSNR = 86.266882
 SSIM = 0.885699
--------------------------------------------------------
--------------------------------------------------------
```

Figure 3.13: Subband 3

```
--------------------------------------------------------
--------------------------------------------------------
Watermarked image Evaluation
 MSE = 9.459981
 PSNR = 88.354567
 SSIM = 0.910503
--------------------------------------------------------
--------------------------------------------------------
```

Figure 3.14: Subband 4

```
--------------------------------------------------------
--------------------------------------------------------
Watermarked image Evaluation
 MSE = 9.858483
 PSNR = 87.941948
 SSIM = 0.897025
--------------------------------------------------------
--------------------------------------------------------
```

Figure 3.15: Subband 5

```
--------------------------------------------------------
--------------------------------------------------------
Watermarked image Evaluation
 MSE = 9.043241
 PSNR = 88.805095
 SSIM = 0.912223
--------------------------------------------------------
--------------------------------------------------------
```

Figure 3.16: Subband 6

The six subbands showed a negligible to no difference in the evaluation metrics results (PSNR, SSIM, MSE). the 6th subband gave the best evaluation results in comparison to the other subbands, and it was selected for the watermarking process.

### 3.4.5 Watermarking Process Evaluation

Here are the comparison results between the original image and the watermarked image after inserting the watermark.
The results are referring to the invisibility of the watermark after the embedding, and referring also to the distortion that effected the original image inserting the watermark.

```
--------------------------------------------------------
--------------------------------------------------------
Watermarked image Evaluation
 MSE = 9.043241
 PSNR = 88.805095
 SSIM = 0.912223
--------------------------------------------------------
--------------------------------------------------------
```

Figure 3.17: Watermarked image evaluation

The data presented in the table convey promising results and show that the DTCWT-SVD preserved the quality of the image from getting distorted.

| | |
|---|---|
| MSE | 9.043241 |
| PSNR | 88.805095 |
| SSIM | 0.912223 |

Table 3.3: Watermarked image evaluation

### 3.4.6 The Attacks on the Watermarking Process

We applied different geometric and processing image attacks on the watermarked image, which are common to affect the image after transmission, in aim to test the robustness of the watermarking method against these operations.

#### 3.4.6.1 Gaussian noise attack

Here is the result of Gaussian noise attack and the source code

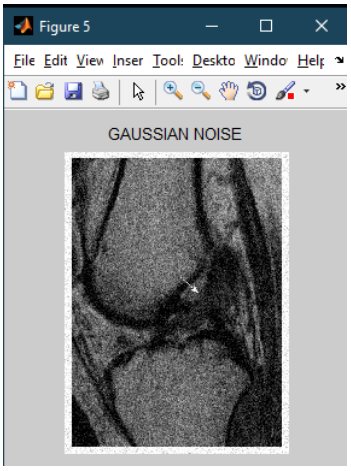


Figure 3.18: Gaussian noise attack

```
1  %% Gaussian Noise Attack
2  function GaussNoiseImageAttacked = noiseGauss(watermarked_image)
3  %watermarked_image = imread(watermarked_image);
4  GaussNoiseImageAttacked = imnoise(watermarked_image, 'gaussian');
5  end
```

Figure 3.19: Gaussian noise attack source code

#### 3.4.6.2 Rotation attack

Here is the result of Rotation attack and the source code

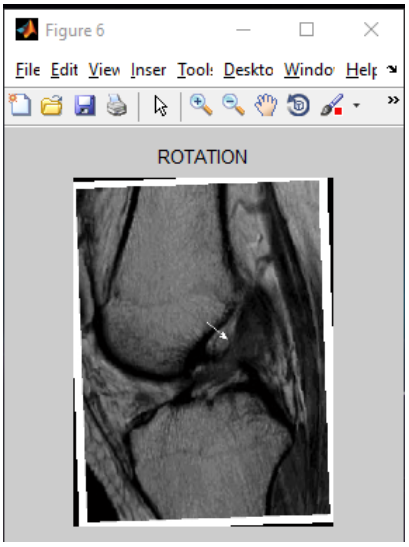


Figure 3.20: Rotation attack

```
%% Rotating Attack 2 degree
function rotatImageAttacked = rotatAttack(watermarked_image)
%watermarked_image = imread(watermarked_image);
rotatImageAttacked = imrotate(watermarked_image, 2,'crop');
end
```

Figure 3.21: Rotation attack source code

#### 3.4.6.3 Average filter attack

Here is the result of Average filter attack and the source code

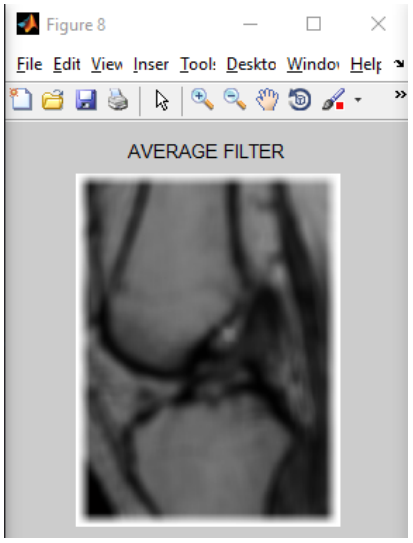


Figure 3.22: Average filter attack

```
%% Average filter Attack
function AverageImageAttacked = averagefilter(watermarked_image)
windowWidth = 21;
kernel = ones(windowWidth) / windowWidth .^ 2;
AverageImageAttacked = imfilter(watermarked_image,kernel,'replicate');
end
```

Figure 3.23: Average filter attack source code

#### 3.4.6.4 Median filter attack

Here is the result of Median filter attack and the source code

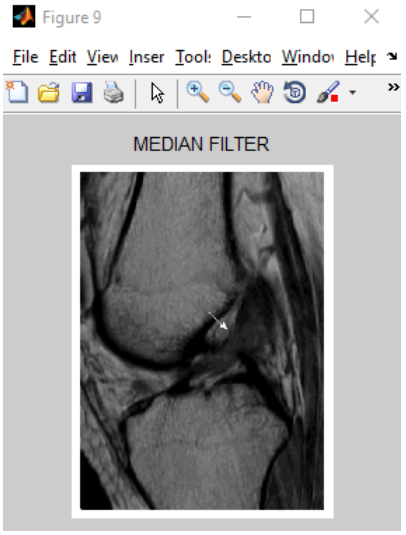


Figure 3.24: Median filter attack

```
%% Median filter Attack
function MedianImageAttacked = medianfilter(watermarked_image)
MedianImageAttacked = medfilt2(watermarked_image);
end
```

Figure 3.25: Median filter attack source code

#### 3.4.6.5 Mean filter attack

Here is the result of Mean filter attack and the source code

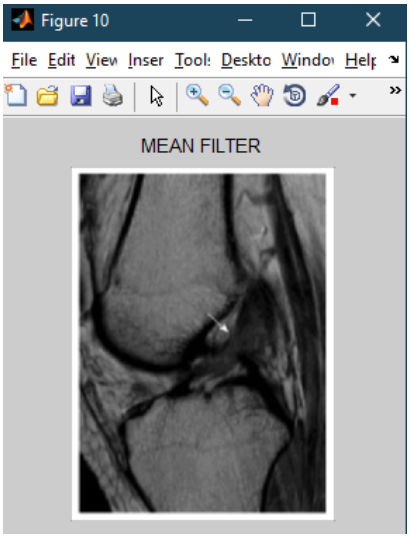


Figure 3.26: Mean filter attack

```
%% Mean filter Attack
function MeanImageAttacked = meanfilter(watermarked_image)
H = fspecial('average', [5 5]);
MeanImageAttacked = imfilter(watermarked_image, H);
end
```

Figure 3.27: mean filter attack source code

#### 3.4.6.6 Salt and pepper noise attack

Here is the result of Salt and pepper noise attack and the source code

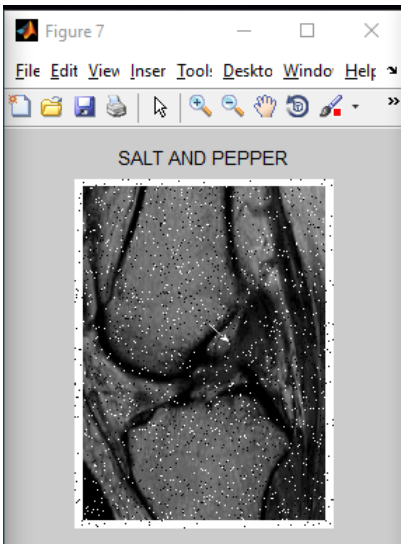


Figure 3.28: Salt and pepper noise attack

```
%% Salt and pepper noise Attack
function GaussNoiseImageAttacked = sandpGauss(watermarked_image)
%watermarked_image = imread(watermarked_image);
GaussNoiseImageAttacked = imnoise(watermarked_image,'salt & pepper');
end
```

Figure 3.29: Salt and pepper noise attack source code

#### 3.4.6.7 Sharpening attack

Here is the result of Sharpening attack and the source code

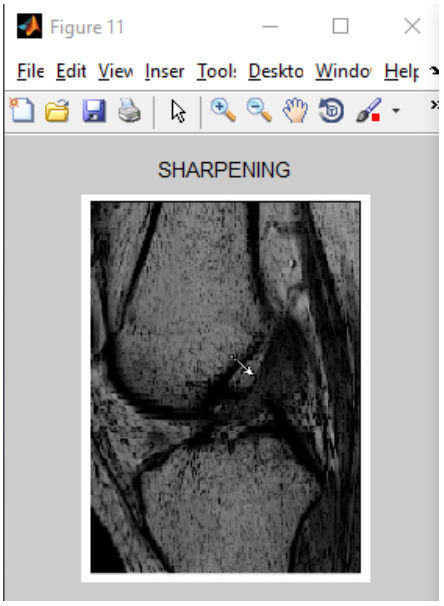


Figure 3.30: Sharpening attack

```
%% Sharpening Attack
function sharpenImageAttacked = sharpen(watermarked_image)
lap = [1 1 1; 1 -8 1; 1 1 1];
resp = uint8(filter2(lap, watermarked_image, 'same'));
sharpenImageAttacked = imsubtract(watermarked_image, resp);
end
```

Figure 3.31: Sharpening attack source code

### 3.4.7 Results of the Attacks

After applying the different attacks we obtained these results :

```
-----------------------------------------------------
Watermaked and attacked watermarked image Evaluation
GAUSSIAN NOISE ATTACK
 MSE = 80.461902
 PSNR = 66.947433
 SSIM = 0.217048
-----------------------------------------------------
ROTATION ATTACK
 MSE = 58.185987
 PSNR = 70.188825
 SSIM = 0.924449
-----------------------------------------------------
SALT AND PEPPER NOISE ATTACK
 MSE = 5.848254
 PSNR = 93.163840
 SSIM = 0.292483
-----------------------------------------------------
AVERAGE FILTER ATTACK
 MSE = 56.799158
 PSNR = 70.430056
 SSIM = 0.977706
-----------------------------------------------------
MEDIAN FILTER ATTACK
 MSE = 2.428177
 PSNR = 101.953863
 SSIM = 0.928918
-----------------------------------------------------
MEAN FILTER ATTACK
 MSE = 15.766786
 PSNR = 83.246215
 SSIM = 0.816841
-----------------------------------------------------
SHARPENING ATTACK
 MSE = 62.207116
 PSNR = 69.520577
 SSIM = 0.720537
-----------------------------------------------------
```

Figure 3.32: Results of the Attacks

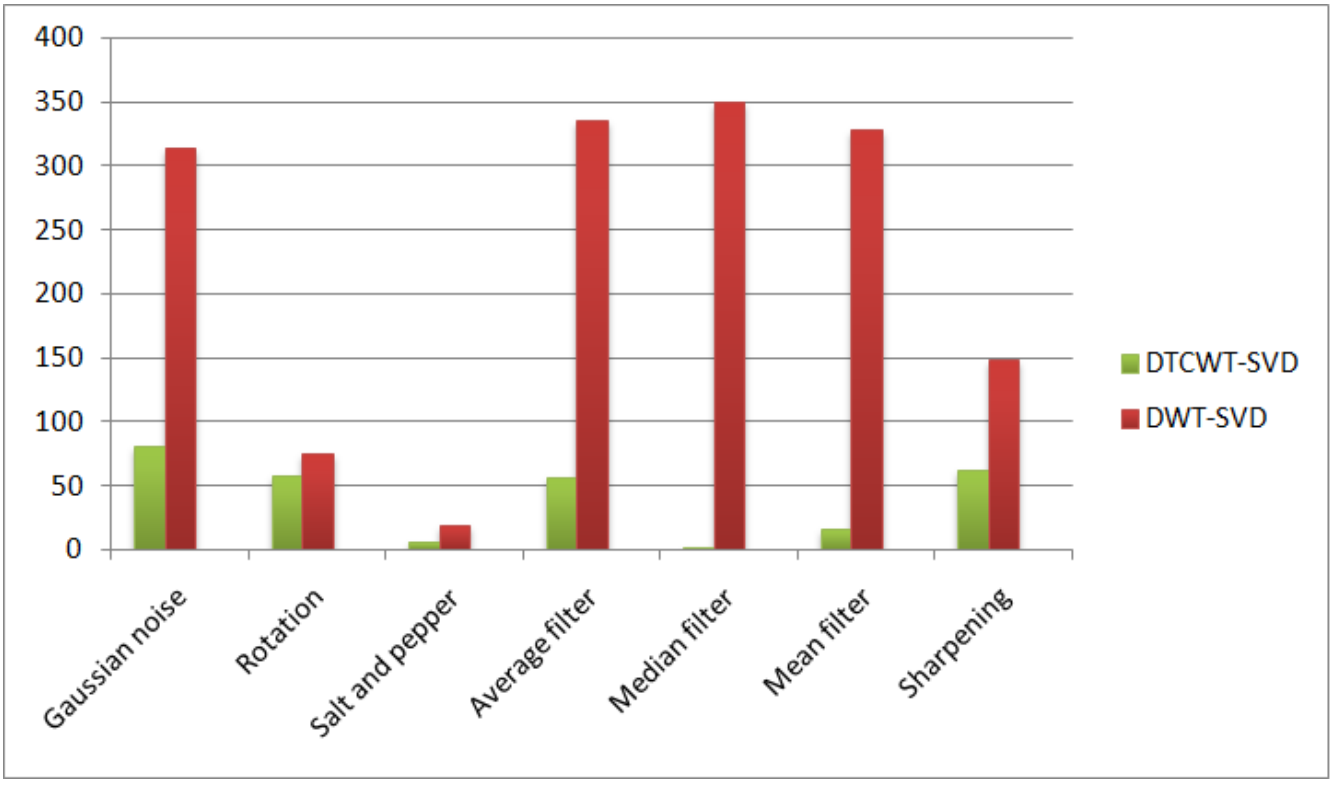


Figure 3.33: MSE Comparison

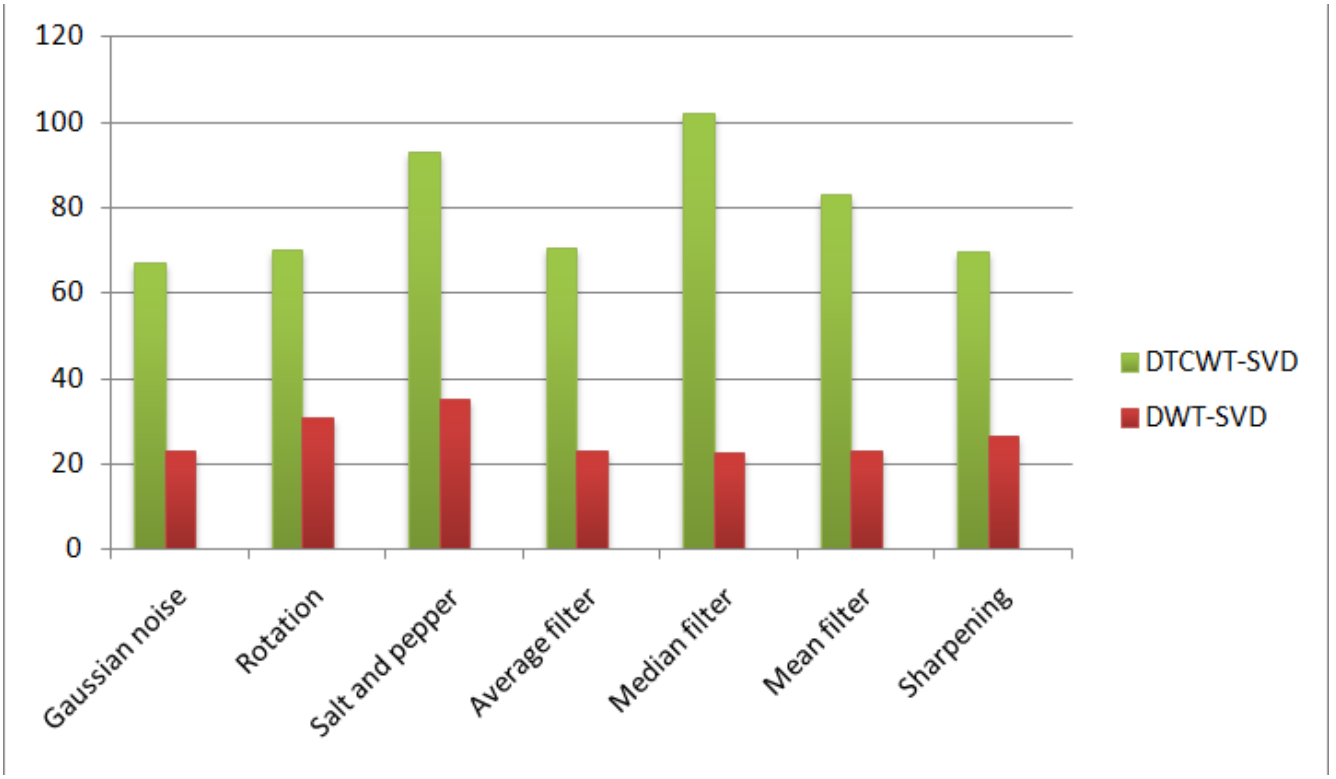


Figure 3.34: PSNR Comparison

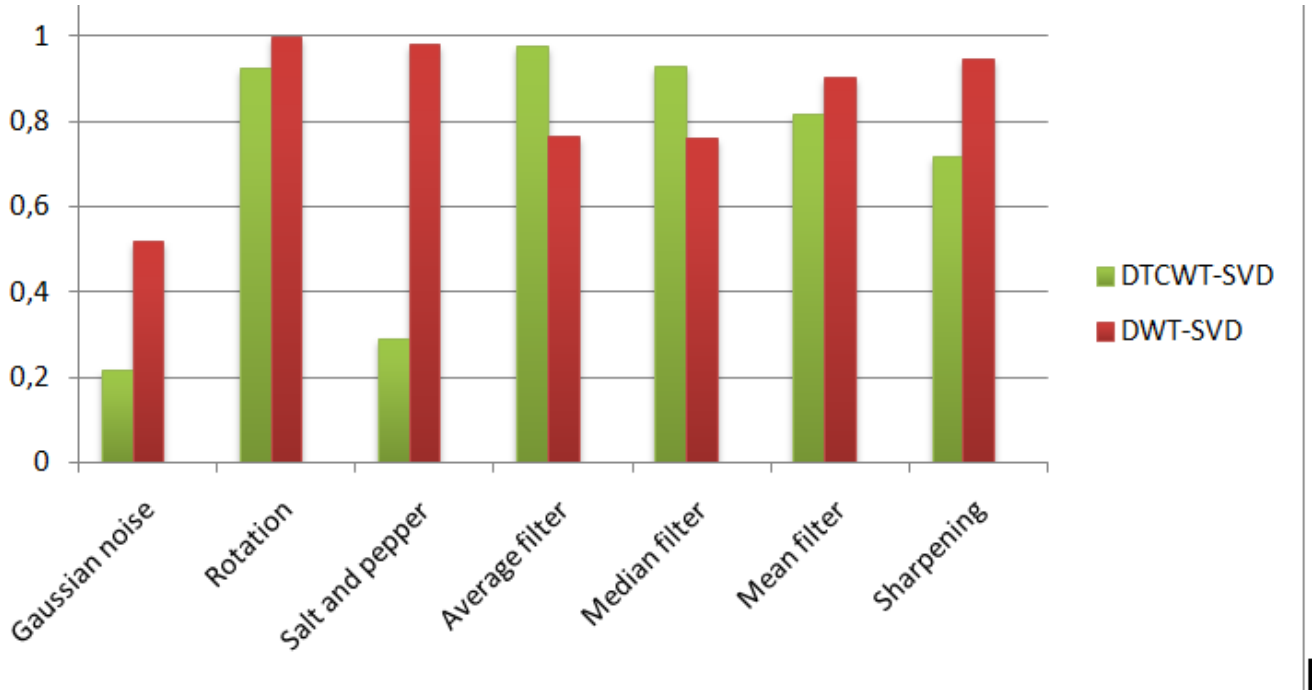


Figure 3.35: SSIM Comparison

The data presented in the MSE, PSNR and SSIM graphs convey promising results and show that the DTCWT-SVD method provides good resistance and robustness against diffrent kinds of common operations in comparison to the results obtained in [68]

## 3.5 Conclusion

The computational results of PSNR, SSIM and MSE using MRI image have a good performance from robustness and imperceptibility points of view. Evaluation results show that the proposed algorithm is robust against geometric distortion and common signal processing operations like filtering and noise addition.
The proposed method avoids a wrong diagnostic caused by image degradation, preserving the imperceptibility requirement for medical images, achieving a PSNR, SSIM and MSE values greater than 88 dB, 0.91 and 9.04, respectively.
We preformed a comparison of methods, and we can conclude that the proposed algorithm outperforms the algorithm proposed in [68] in terms of imperceptibility and robustness, which is one of the most efficient algorithms proposed in the literature of watermarking.

# CONCLUSION

In this thesis, a blind watermarking scheme based on Dual Tree Complex Wavelet Transform was proposed. This included the advantages of both multi wavelet and complex representation of an image.

Eigen values (SV's) of the selected host subband are modified by the Eigen values of selected subband of the watermark. During extraction process, watermark was extracted with the help of strength factor there was no need of the original host and watermark for extraction.

Experimental results show that the proposed algorithm produced a high imperceptibility and a high robustness against various kinds of attacks like median filtering, mean filtering, rotation, sharpening and addition of noise like Gaussian, Salt and Pepper, Speckle.

From the results of comparison with existing methods, we can observe that the proposed watermarking scheme achieves better imperceptibility and robustness in the medical watermarking field.

# BIBLIOGRAPHY


[1] J.A. Seibert. *"Archiving, Chapter 2: Medical Image Data Characteristics - Society for Imaging Informatics in Medicine," SIIM.org.*

[2] C. Nait-Ali Cavaro-Ménard. *A. "Compression des images et des signaux médicaux, " HERMES, Lavoisier, Vuibert, Paris.* 2007.

[3] J. A. Leidholdt E. M. Boone J. M. Goldschmidt E. J Bushberg, J. T. Seibert. *"The essential physics of medical imaging." Medical Physics 30, 1936–1936.* 2003.

[4] Bernard Mazoyer Guy Frija, Clara Delpas. *Imagerie médical . Fondation pour la Recherche Medical.* www.from.orgClara Delpas, 2002.

[5] Y.Q.; Wang X.D.; Ji S.J Yang, H.M.; Liang. *A DWT-Based Evaluation Method of Imperceptibility of Watermark in Watermarked Color Image.* In Proceedings of the 2007 International Conference on Wavelet Analysis and Pattern Recognition.

[6] H Zhang, F.; Zhang. *Digital Watermarking Capacity and Reliability.* In Proceedings of the IEEE International Conference on e-Commerce Technology.

[7] B.P Kavitha, K.J.; Shan. *Implementation of DWM for Medical Images using IWT and QR Code as a Watermark.* In Proceedings of the IEEE Conference on Emerging Devices and Smart System.

[8] Mohammad Shorif Uddin Mahbuba Begum. *Digital Image Watermarking Techniques: A Review.* 2020.

[9] B. Sankur Y. Rolland R. Collorec G. Coatrieux, H. Maitre. *"Relevance of watermarking in medical imaging,".* in Information Technology Applications in Biomedicine, 2000. Proceedings. 2000 IEEE EMBS International Conference on, 2000, pp. 250-255.

[10] S. Das and M. Kundu. *"Effective Management of Medical Information Through A Novel Blind Watermarking Technique,".* Journal of Medical Systems, pp. 1-13.

[11] K.A. Navas and M. Sasikumar. *"Survey of Medical Image Watermarking Algorithms,".* presented at the 4rth International Conference: Sciences of Electronic, Technologies of Information and Telecommunications (SETIT ), TUNISIA, 2007.

[12] C.-M. Hsu H.-M. Chao and S.-G. Miaou. *"A data-hiding technique with authentication, integration, and confidentiality for electronic patient records,"*. IEEE Transactions on Information Technology in Biomedicine, vol. 6, pp. 46-53, 2002.

[13] D. Megias M. Fallahpour and M. Ghanbari. *"High capacity, reversible data hiding in medical images,"*. in Image Processing (ICIP), 2009 16th IEEE International Conference on, 2009, pp. 4241-4244.

[14] M. K. Kundu and S. Das. *"Lossless ROI Medical Image Watermarking Technique with Enhanced Security and High Payload Embedding,"*. in Pattern Recognition (ICPR), 2010 20th International Conference on, 2010, pp. 1457-1460.

[15] G. Ulutas M. Ulutas and V. V. Nabiyev. *"Medical image security and EPR hiding using Shamir's secret sharing scheme," Journal of Systems and Software, vol. In Press, Corrected Proof.* 2010.

[16] H. Chen Z.-L. Huang H. Li H. Luo, F.-X. Yu and P.-H. Wang. *"Reversible data hiding based on block median preservation," Information Sciences, vol. 181, pp. 308-328.* 2011.

[17] C.-J. Chen C.-L. Wang T.-H. Kuo W. K. Moon J. H. K. Wu, R.-F. Chang and D.-R. Chen. *"Tamper detection and recovery for medical images using near-lossless information hiding technique," Journal of Digital Imaging, vol. 21, pp. 59-76.* 2008.

[18] Y. Yuanyuan L. Chenwen-Y. Yihong J. Jin C. Weihua-S. Kun Z. Jianguo, S. Jianyong and Z. Guozhen. *"Image-based electronic patient records for secured collaborative medical applications,"*. in 2005 27th Annual International Conference of the IEEE Engineering in Medicine and Biology Society, 31 Aug.-3 Sept. 2005, Piscataway, NJ, USA, 2006, p. 3 pp.

[19] A. Schröter H. Münch, U. Engelmann and H. P. Meinzer. *"The integration of medical images with the electronic patient record and their web-based distribution1,"*. Academic Radiology, vol. 11, pp. 661-668, 2004.

[20] D. K. W. Chiu S.-C. Cheung and C. Ho. *"The Use of Digital Watermarking for Intelligence Multimedia Document Distribution," Journal of theoretical and applied electronic commerce research, vol. 3, pp. 103-118,.* 2008.

[21] T. Rockwood W. Zhou and P. Sagetong. *"Non-repudiation oblivious watermarking schema for secure digital video distribution," in Multimedia Signal Processing, 2002 IEEE Workshop on.* 2002, pp. 343-346.

[22] J. Fridrich. *"Applications of data hiding in digital images," in Proceedings of Fifth International Symposium on Signal Processing and its Applications, 22-25 Aug. 1999, Brisbane, Qld., Australia,.* 1999, p. 9 vol.1.

[23] S. Archana Thampy K. A. Navas and M. Sasikumar. *"EPR Hiding in Mecial Images for Telemedicine," in Proceedings of World Academy of Science and Engineering and Technology.* 2008.

[24] Garima Singh. *A review of secure medical image watermarking.* 2017.

[25] Nour El-Houda GOLEA. *GOLEA Approches Evolutionnaires Hybrides pour Le Tatouage Numérique des Images.*

[26] Sugata Sanyal Tanmoy Sarkar. *Reversible and Irreversible Data Hiding Technique.*

[27] Kai-Kuang Ma Dan Yu, Farook Sattar. *Watermark Detection and Extraction Using Independent Component Analysis Method.* 2002.

[28] Anis Sakly Seifeddine Naffouti, Hayet Homri and Abdellatif Mtibaa. *An additive image watermarking method based on particle swarm optimization.*

[29] A Habes. *Information Hiding in BMP Image Implementation, Analysis and Evaluation. Inf. Transm. Comput. Netw.* 2006, 6, 1–10.

[30] A. A. Manaf A. M. Zeki and S. a. S. Mahmod. *"Analysis of ISB watermarking model: block based methods vs embedding repetition methods,".* presented at the Proceedings of the 9th International Conference on Advances in Mobile Computing and Multimedia, Ho Chi Minh City, Vietnam, 2011.

[31] R. Rathor, B.; Saharan. *Steganography using Bit Plane Embedding and Cryptography. In Proceedings of the 1st International Conference on Smart System, Innovations and Computing, Jaipur, India, 2018; Volume 79, pp. 319–330.*

[32] Shobha Elizabeth Rajan Sreedevi P. *A Survey On Wavelet Domain Watermarking.*

[33] Y.; Hu W.; Qian D Chen, Z.; Chen. *Wavelet Domain Digital Watermarking Algorithm Based on Threshold Classification.*

[34] C.H.; Swamy K.V. Haribabu, M.; Bindu. *A Secure Invisible Image Watermarking Scheme Based on Wavelet Transform in HSI color space.*

[35] Rita Choudhary Girish Parmar. *A Robust image Watermarking Technique using 2-level Discrete Wavelet Transform.*

[36] N.Nikolaidis. *ARobust image watermarking in the spatial domain.*

[37] Eric Garcia Mohamed Salim BOUHLEL Imen Fourati Kallel, Mohamed Kallel. *Fragile Watermarking for medical Image Authentication.*

[38] Sun Xie-hua Zhao Yang. *A Semi-fragile Watermarking Algorithm based on HVS Model and DWT.*

[39] *Application de la theorie des ondelettes valerie perrier.* 2015.

[40] Patrick Loo. *Digital Watermarking using Complex Wavelets.*

[41] Panchamkumar D SHUKLA. *CWT and their applications.*

[42] *Nick Kingsbury. Image processing with complex wavelets. Philosophical Transactions of the Royal Society London.*

[43] R. Baraniuk I. Selesnick and N. Kingsbury. *The dual-tree complex wavelet transform.*

[44] N.G. Kingsbury. *The dual-tree complex wavelet transform : A new efficient tool for image restoration and enhancement.*

[45] N.G. Kingsbury. *A dual-tree complex wavelet transform with improved orthogonality and symmetry properties.*

[46] I.W. Selesnick. *The design of approximate hilbert transform pairs of wavelet bases.*

[47] T. Will. *"Introduction to the Singular Value Decomposition," vol. 2006: UW-La Crosse.* 1999.

[48] and AZAR F. Mansouri A, Aznaveh A. M. *" SVD Based Digital Image Watermarking Using Complexwavelet Transform ",Department Of Electrical and Computer Engineering Shahid Beheshti University.* 2009.

[49] Varga R. Smithies L. *" Singular Value Decomposition ", Department Of Mathematical Sciences , Kent State University ,Kent, Ohio, U.S.A.* 2009.

[50] Sheriff M S. *" Analyzing Software Artifacts Through Singular Value Decomposition to Guide Development Decisions", North Carolina State University, Computer Science.* 2007.

[51] R. Liu and T. Tan. *An SVD-Based Watermarking Scheme for Protecting Rightful Ownership. In IEEE Transactions on Multimedia, volume 4, pages 121–128] – 67.* March 2002.

[52] C.T. Hsu and J.L.WU. *" Hidden digital watermarks in images" ,IEEE Transactions Trans actions on Image Processing ,vol.8,no.1,pp.58-68.* 1999.

[53] Sura Ramzi Sheriff. *Digital Image Watermarking Using Singular Value Decomposition.* 2010.

[54] Chang C. C. *"An SVD Oriented Watermark Embedding Scheme With High Qualities For The Restored Images", Department of Information Engineering and Computer Science, Feng Chia University, Taiwan.* 2007.

[55] Mahbuba Begum and Mohammad Shorif Uddin. *Digital Image Watermarking Techniques: A Review.* 2020.

[56] M. Zamani T. K. Araghi, A. B. A. Manaf and S. Araghi. *"A Survey on Digital Image Watermarking Techniques in Spatial and Transform Domains," Third International Conference on Advances In Computing, Control And Networking - ACCN 2015.* 2015.

[57] *https://www.mathworks.com/discovery/what-is-matlab.html.* accessed 08/06/2022.

[58] D. Chonacky, N.; Winch. *"Reviews of Maple, Mathematica, and Matlab: Coming Soon to a Publication Near You". Computing in Science Engineering. Institute of Electrical and Electronics Engineers (IEEE). 7 (2): 9–10.* 2005.

[59] Thomas. Haigh. *"Cleve Moler: Mathematical Software Pioneer and Creator of Matlab" (PDF). IEEE Annals of the History of Computing. IEEE Computer Society.*

[60] Jack Moler, Cleve; Little. *"A history of MATLAB". Proceedings of the ACM on Programming Languages. Association for Computing Machinery (ACM). 4 (HOPL): 1–67.* June 12, 2020.

[61] T.U. Xue, D.; Press. *MATLAB Programming: Mathematical Problem Solutions. De Gruyter STEM. De Gruyter. p. 21.* 2020.

[62] CRC Press. *Solving Applied Mathematical Problems with MATLAB. CRC Press. p. 6. ISBN 978-1-4200-8251-7.* 2008.

[63] C. Woodford, C.; Phillips. *Numerical Methods with Worked Examples: Matlab Edition. SpringerLink : Bücher. Springer Netherlands. p. 1.* 2011.

[64] J.V. Tranquillo. *MATLAB for Engineering and the Life Sciences. Synthesis digital library of engineering and computer science. Morgan  Claypool Publishers.* 2011.

[65] Lori LoTurco. *"Accelerating the pace of engineering". MIT News. Massachusetts Institute of Technology.* January 28, 2020.

[66] *https://www.mathworks.com/help/matlab/release-notes.html.* accessed 23/06/2022.

[67] *Mean Squared Error. In: Sammut, C., Webb, G.I. (eds) Encyclopedia of Machine Learning. Springer, Boston, MA.* 2011.

[68] Prof. Dr. Farkhand Shakeel Mahmood Nouman Shah Hamza Bin Tahir-Hassan Malik Saira Mudassar, Munazah Jamal. *Hybrid DWT-SVD Digital Image Watermarking.*